Inhalt

17.09.13	Begrüssung & Laborführung
24.09.13	Nanostructuring 1 (Oberflächendiffusion)
01.10.13	Nanostructuring 2 (Selbst-Organisation, Substrate „Template“ Effekte)
08.10.13	Frei
15.10.13	Analysemethoden 1 (Rastertunnel- und Rasterkraft-Mikroskopie)
22.10.13	Analysemethoden 2 (dynamic AFM, SIMS und TOF-SIMS)
29.10.13	Analysemethoden 3 (Photoemissions- und Augerspektroskopie)
05.11.13	Deposition Techniques 1 (Graphene Herstellung und Analyse)
12.11.13	Deposition Techniques 2 (Ionenstrahltechnik, Plasma)
19.11.13	Deposition Techniques 3 (Verdampfung, MBE, PVD, CVD, OVPD)
26.11.12	Lithographie und Ätzprozesse (Elektronenstrahllithographie)
03.12.13	Kolloidale Methoden und inverse Mizellen
10.12.13	Growth nanotubes and graphene
17.12.12	Präsentationen

Nanostrukturen-Analysemethoden

Scanning Probe Microscopy

- **Scanning Tunneling Microscopy**
- Tunnel Current
- G. Binnig and H. Rohrer, Nobelpreis 1986
- Experimental Setup
- **Friction Force Microscopy**
- Force Calibration
- Atomic Stick Slip
- Tomlinson Model
- Nano-manipulation
- **Atomic Force Microscopy**
- Short- and Long-Range Forces
- Kelvin Probe Force Microscopy
- Measurements on Semiconducting Devices
- Molecules on Insulating Surfaces
- Manipulation

Thilo Glatzel, thilo.glatzel@unibas.ch
NANOlino Lab

„Beam deflection“-Methode

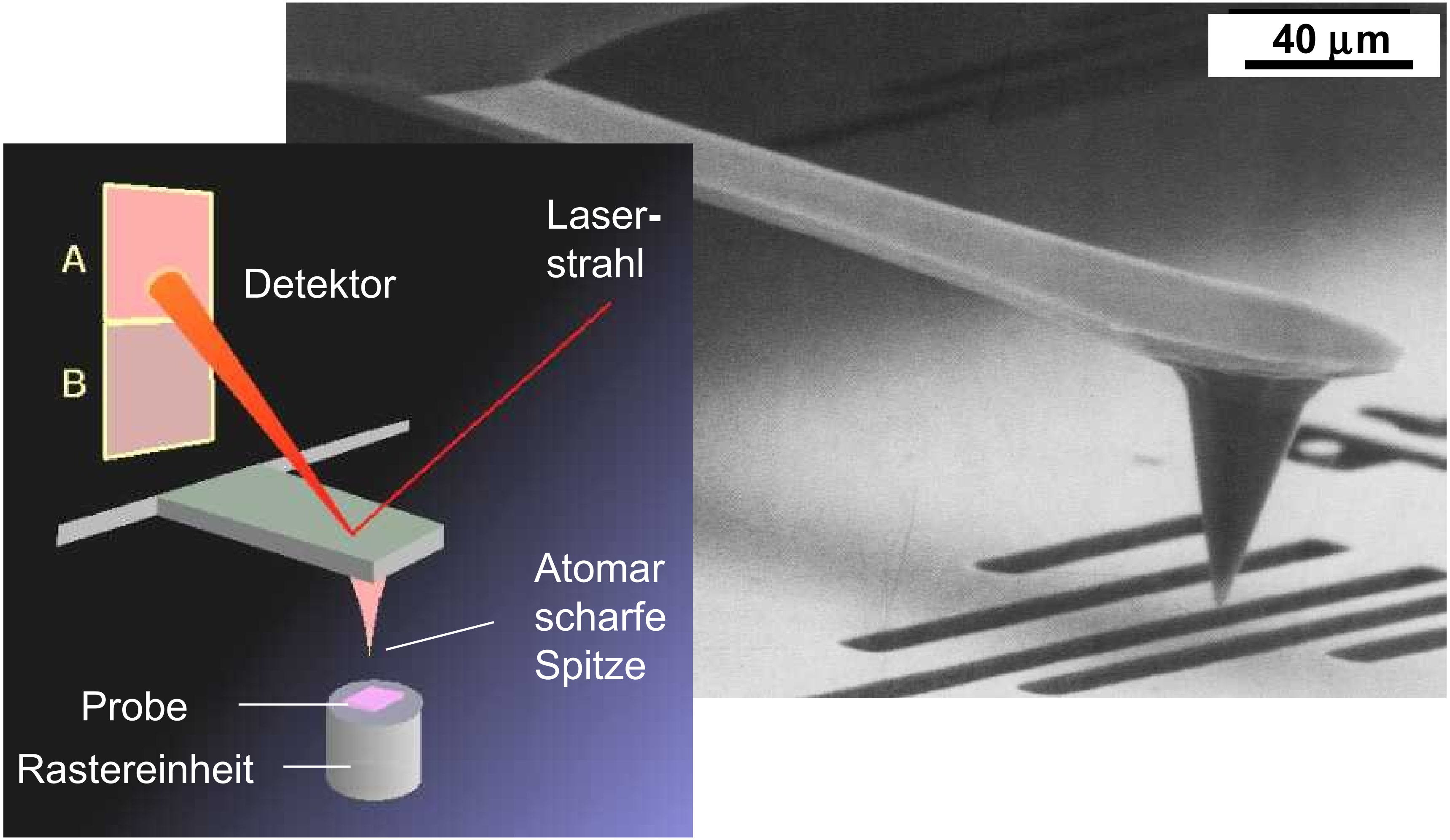

contact and dynamic AFM

Wieviel Kraft braucht man für einen molekularen Schalter?

Noncontact-AFM (nc-AFM)

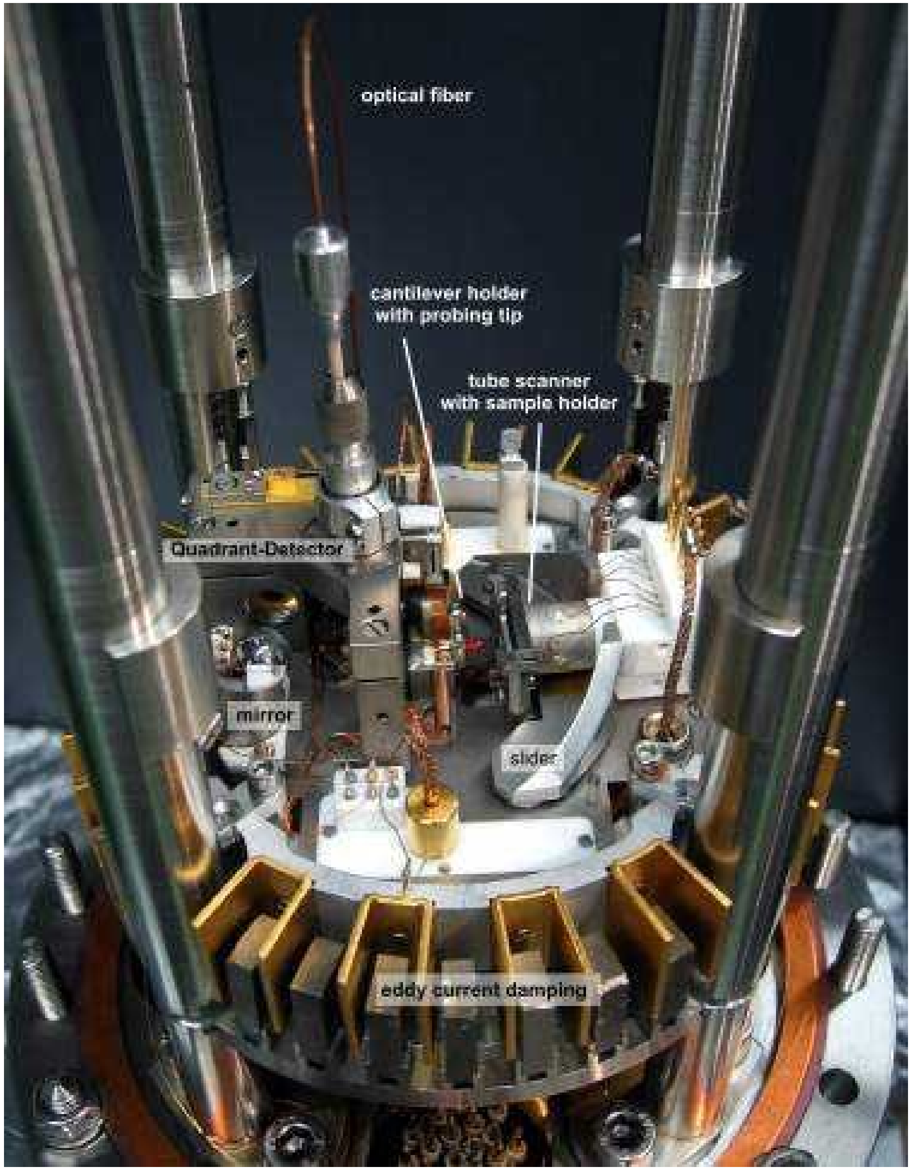

- UHV: Base pressure below 1×10^{-10} mbar
- Operation at room temperature
- Mixed mode: AFM/STM
- Beam deflection method
- Bandwidth of the photodetector: 3MHz
- Evaporation of molecules from a k-cell kept at 165ºC or 170ºC

Quantitative understanding of nc-AFM

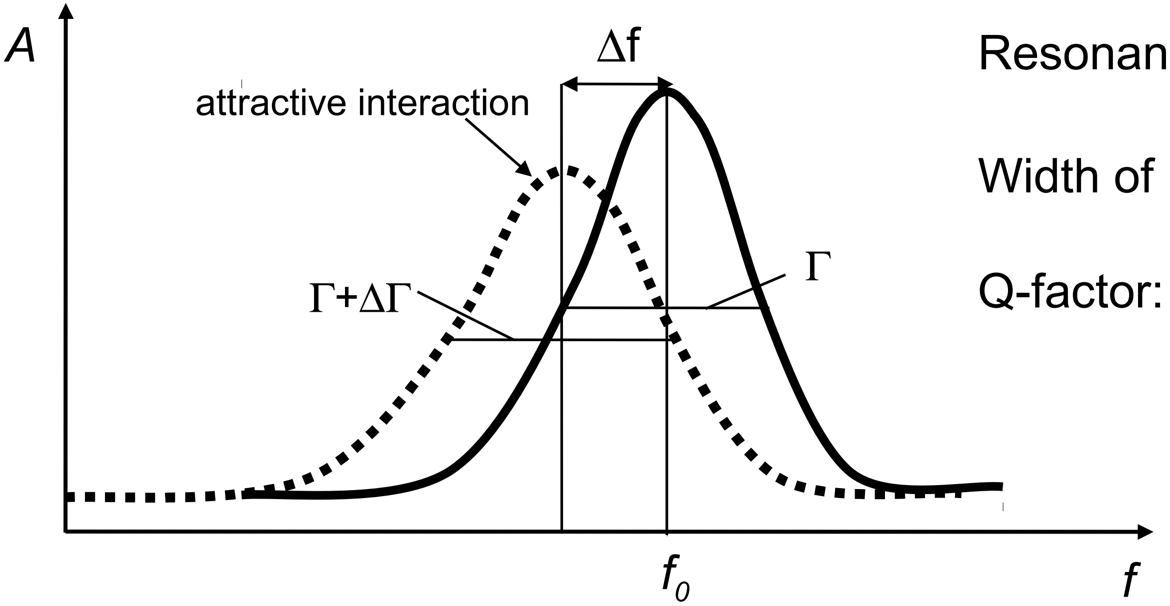

Resonance frequency: f_0

Width of resonance curve (FWHM): Γ

Q-factor: $Q = \frac{2\pi \cdot f_0}{\Gamma}$

Conservative forces ⇒ shift of resonance curve Δf
Dissipative forces ⇒ broadening of curve $\Delta\Gamma$

Forces in nc-AFM

Frequency modulation: $f_0 = \frac{1}{2\pi}\sqrt{\frac{k}{m^*}}$ $\Delta f = -\frac{f_0}{2k}\frac{\partial F_{tot}}{\partial z}$

$\Rightarrow$ measured topography = surface of constant $\frac{\partial F}{\partial z}$

$$F_{tot} = F_{chem} + F_{mag} + F_{el} + F_{vdW}$$

bonding between tip and sample atoms (only for d < 5 Å)

only for magnetically sensitive tips

$$F_{el} = -\frac{1}{2}\frac{\partial C}{\partial z}V^2$$

$$F_{vdW} = -\frac{HR}{6d^2}$$

Dynamic Mode, non-contact

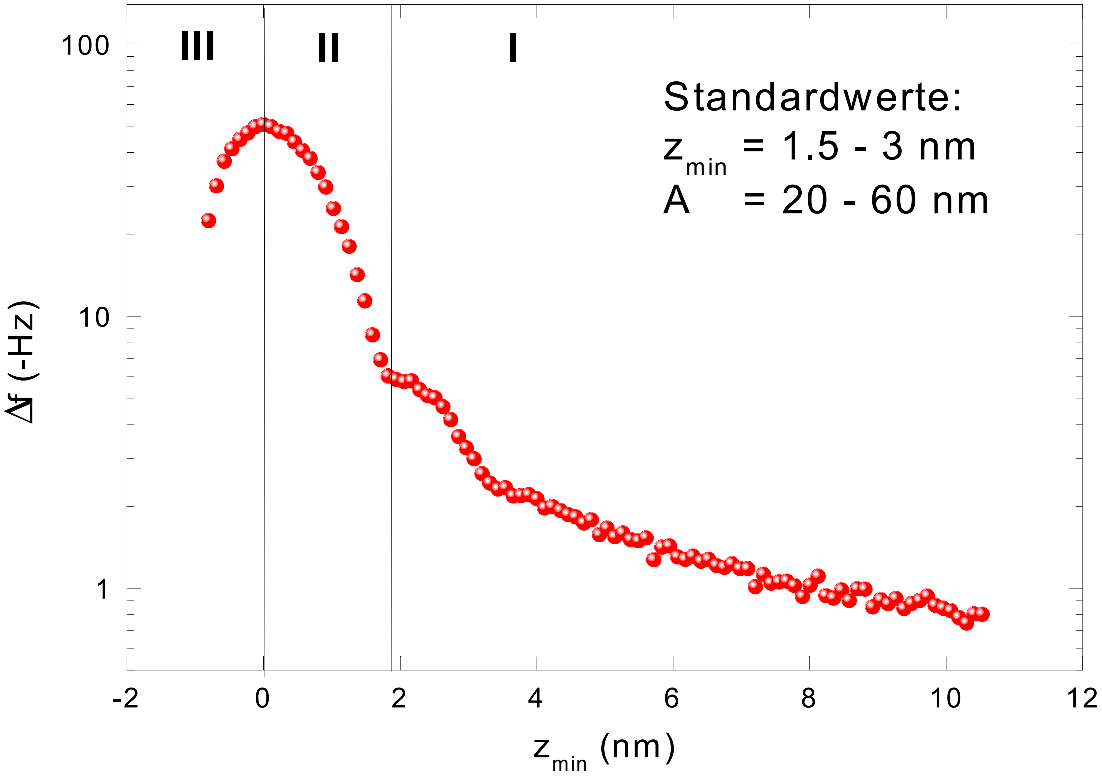

region I:
attractive forces
non-contact mode

region II:
attractive forces
atomic resolution

region III:
repulsive forces
tapping mode

Short range interaction

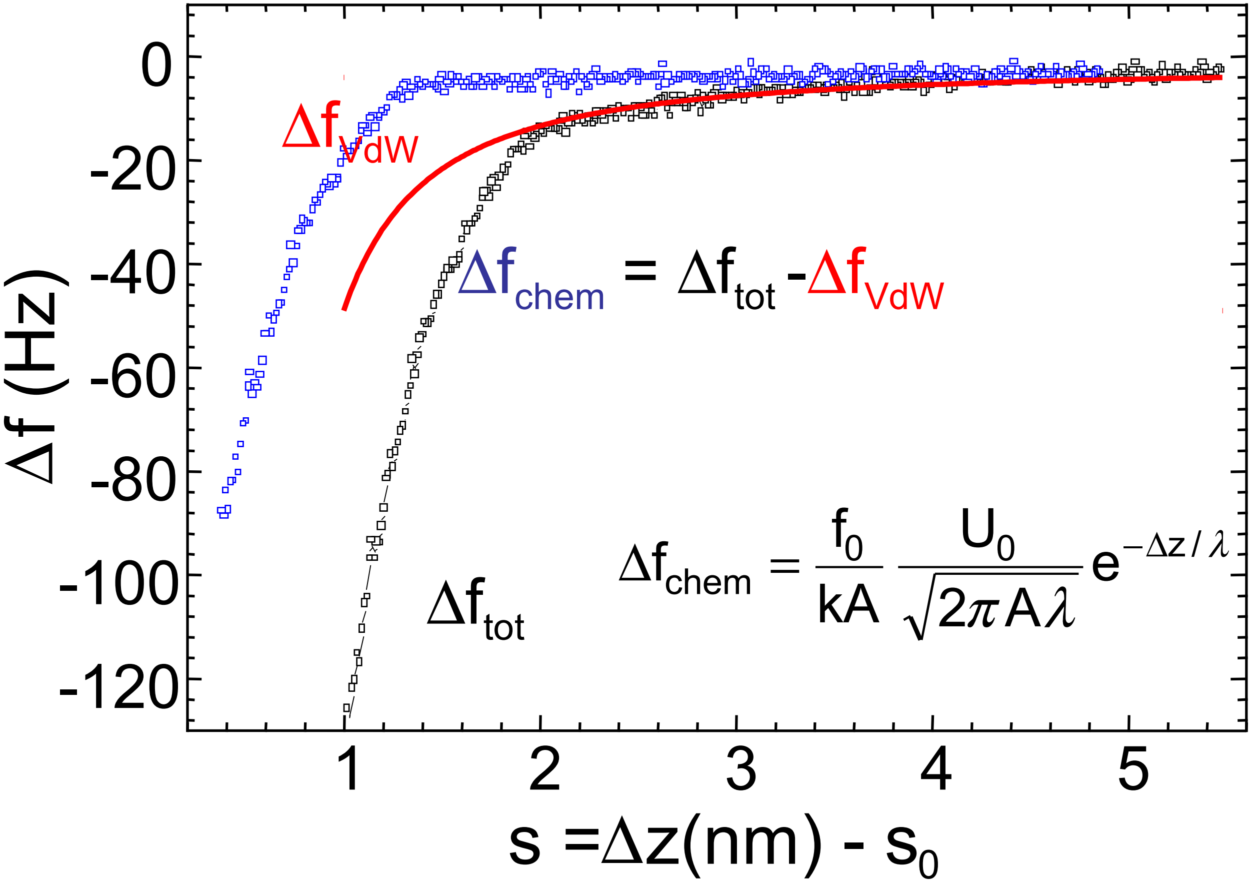

$\lambda = 0.35$ nm

$U_0 = -4.7$ eV

$s_0 = 0.45$ nm

Carbon nanotubes as probing tips for nc-AFM

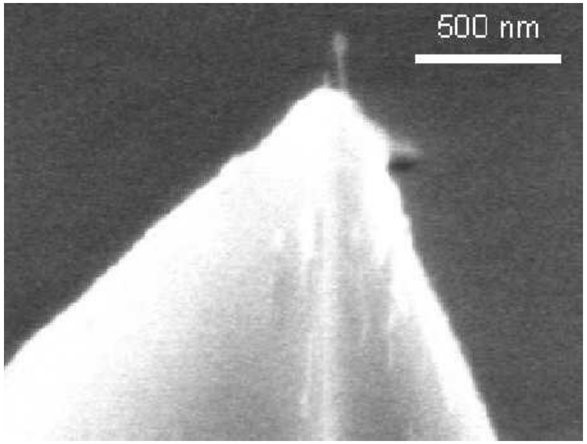

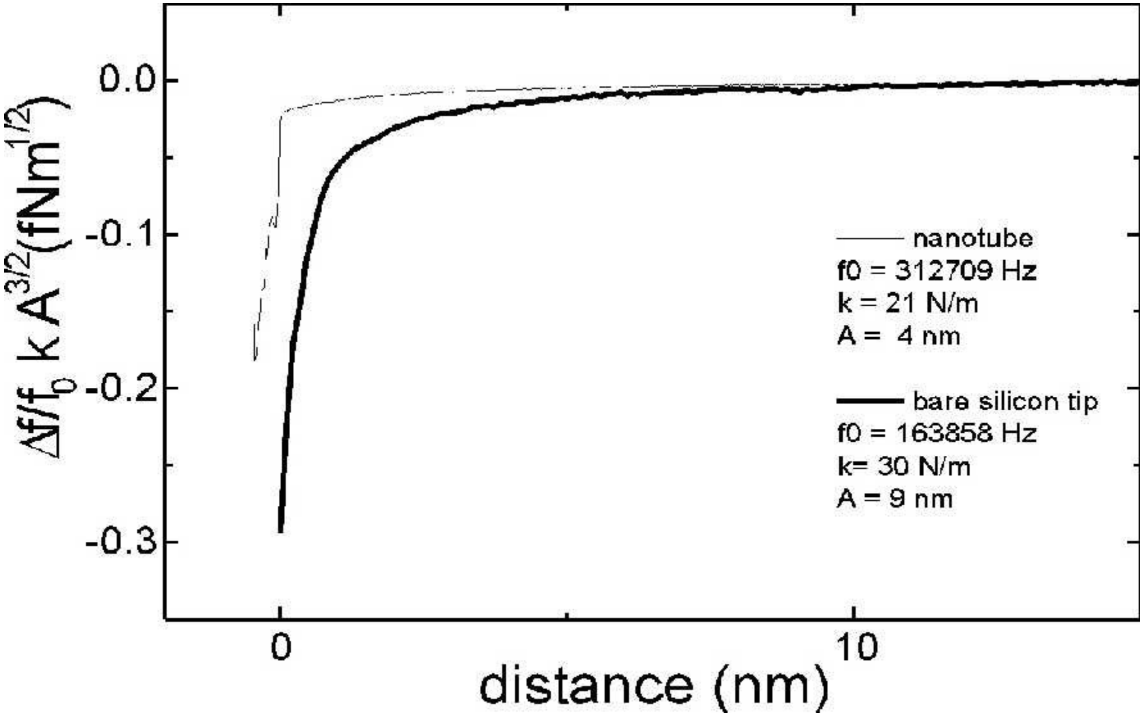

⇒ Long-range forces are reduced

inhomogeneous sample: HOPG + ½ monolayer C60

Topography

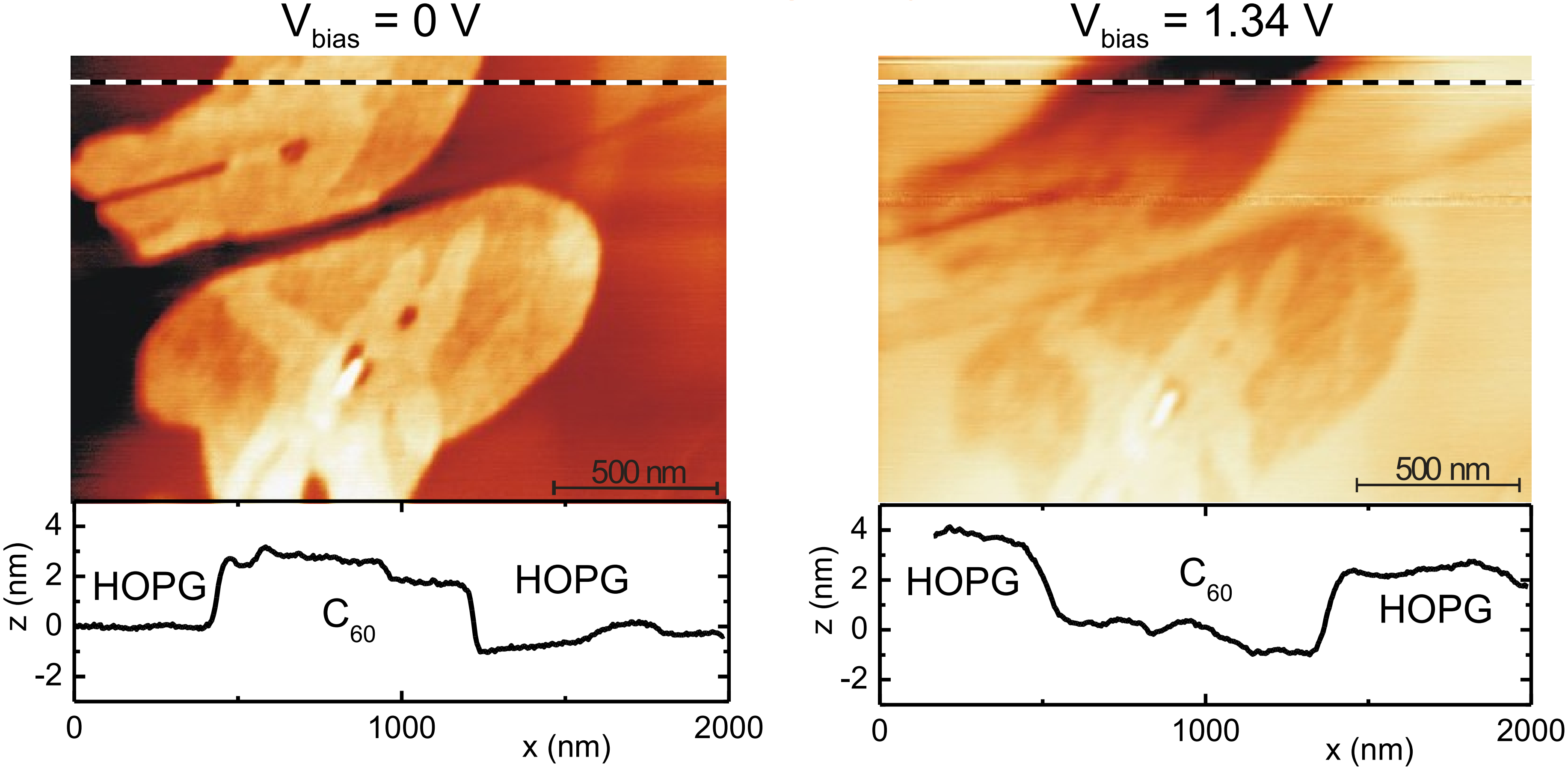

→ contrast inversal: HOPG ↔ C_{60}

S. Sadewasser et al., PRL 91 266101 (2003)

inhomogeneous sample: HOPG + ½ monolayer C60

topography

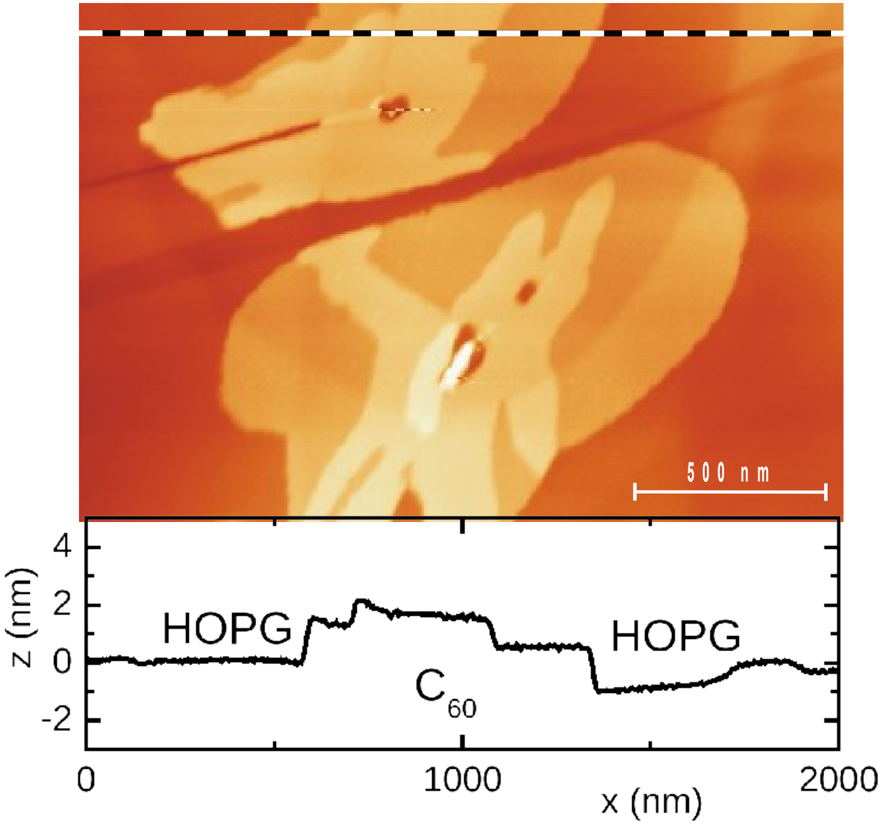

contact potential

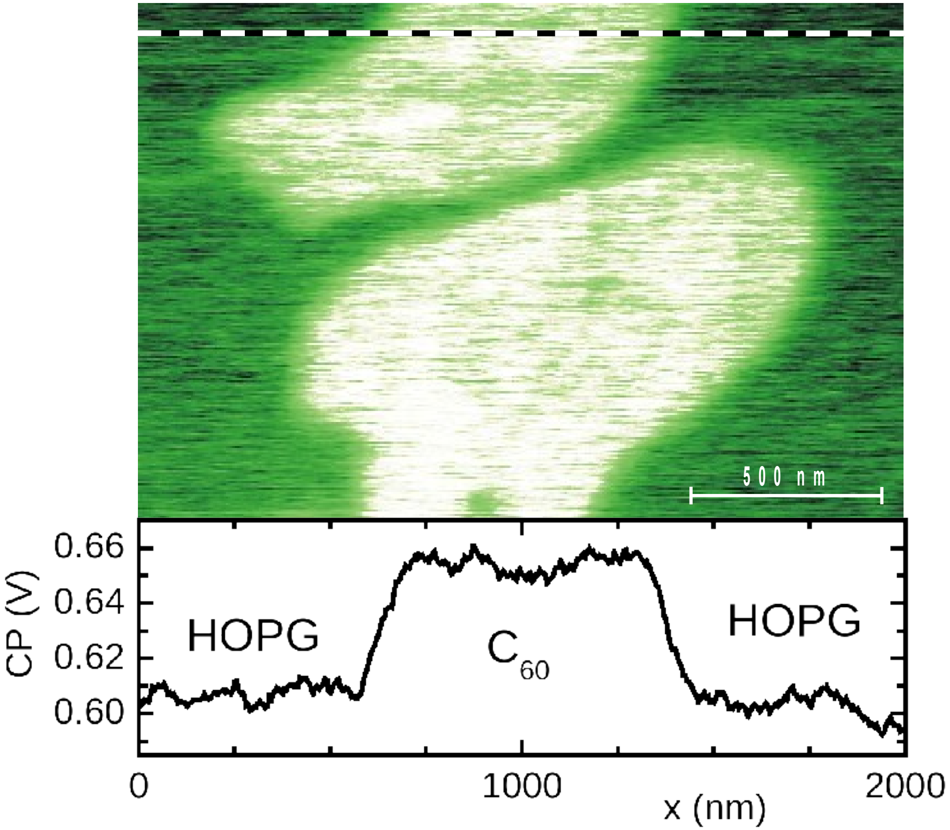

HOPG: $V_{CP} \cong 0.61$ V

C_{60}: $V_{CP} \cong 0.66$ V

⇒ NC-AFM: residual electrostatic force for fixed V_{bias}

Makroskopische Kelvin-Sonde

Lord Kelvin 1861

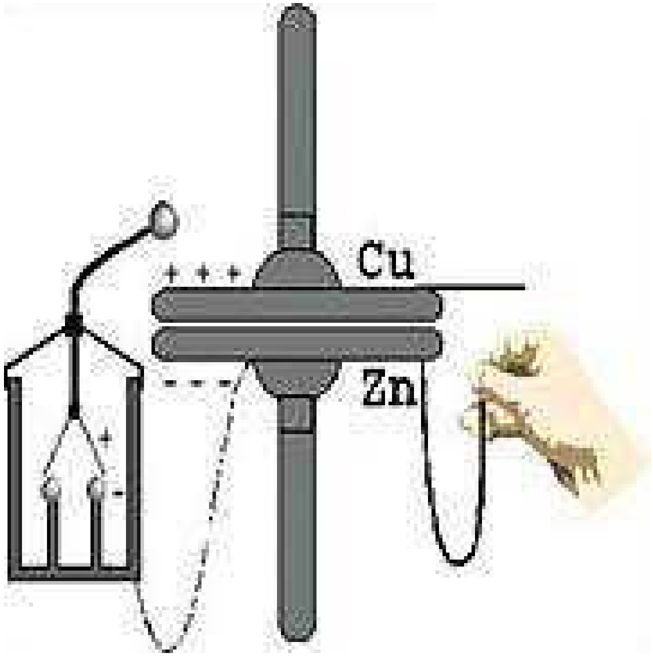

Verschiebestrom

$I(t) = (U_{dc} - U_{CPD})\, f\ \Delta C \cos \omega t.$

Kelvin Principle

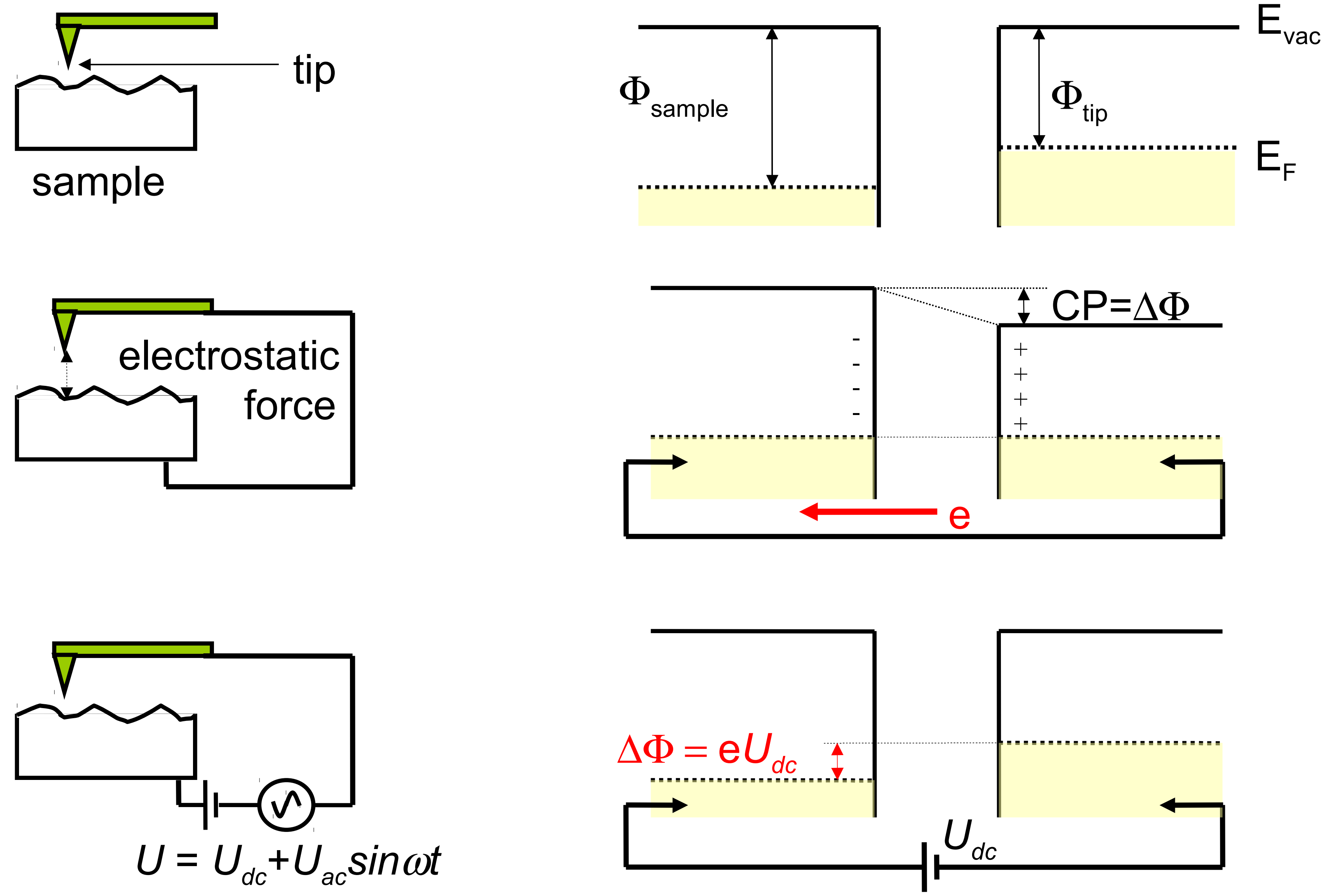

Electrostatic Forces in nc-AFM

$$F_{el} = \frac{1}{2}\frac{\partial C}{\partial z}V_{eff}^{2} \quad \Rightarrow \quad F_{el} = \frac{1}{2}\frac{\partial C}{\partial z}\left(V_{bias} - V_{CP}\right)^{2}$$

$$V_{CP} = 1/e \cdot \left(\Phi_{tip} - \Phi_{sample}\right)$$

contact potential

Φ - work function

apply bias: $\boxed{V_{bias} = V_{dc} + V_{ac} \cdot \sin(\omega t)}$

Kelvin Probe Force Microscopy

$$F_{el} = \frac{1}{2}\frac{\partial C}{\partial z}V_{eff}^{2} = F_{dc} + F_{\omega} + F_{2\omega}$$

$$F_{dc} = \frac{\partial C}{\partial z}\left[\frac{1}{2}\left(V_{dc} - V_{CP}\right)^{2} + \frac{V_{ac}^{2}}{4}\right]$$

$$F_{\omega} = \frac{\partial C}{\partial z}\left(V_{dc} - V_{CP}\right)V_{ac}\sin(\omega t)$$

$$F_{2\omega} = -\frac{\partial C}{\partial z}\frac{V_{ac}^{2}}{4}\cos(2\omega t)$$

AM-KPFM

Amplitude Modulation

FM-KPFM

Frequency Modulation

FM – KPFM
Frequency Modulation Detection

$$\Delta f(\omega) \propto \frac{\partial F_{el}}{\partial z} \propto \frac{\partial^2 C}{\partial z^2}\left(V_{dc} - V_{CP}\right) V_{ac} \sin(\omega t)$$

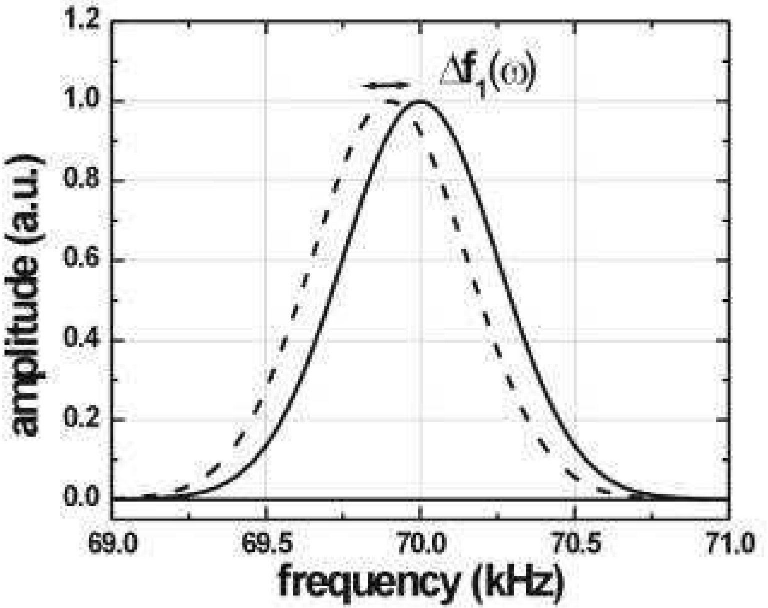

- frequency ω of V_{ac} between 1-3 kHz
- detection of the oscillation of $A(\Delta f_1)$ with a lock-in
- limiting factor: bandwidth of the FM-demodulator / PLL

$$A(\Delta f_1) \propto \partial F_{el}/\partial z$$

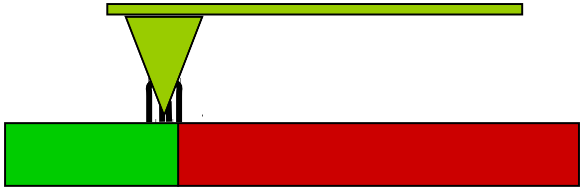

AM – KPFM
Amplitude Modulation Detection

$$F_{\omega} = -\frac{\partial C}{\partial z}\left(V_{dc} - V_{CP}\right) V_{ac} \sin(\omega t)$$

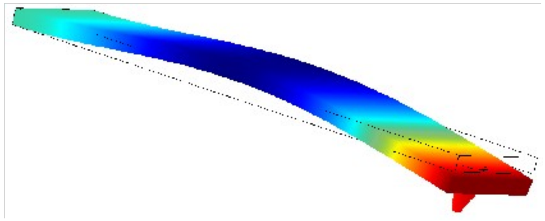

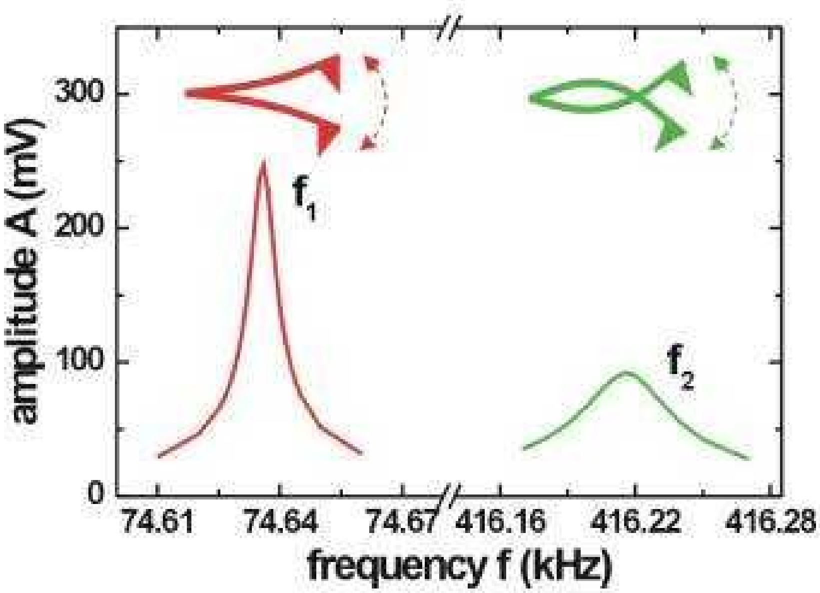

- tune ω to the second resonance f_2
- detection of the oscillation amplitude A_{ω} with a lock-in
- limiting factor: bandwidth of the photodiode

$$A_{\omega} \propto F_{\omega}$$

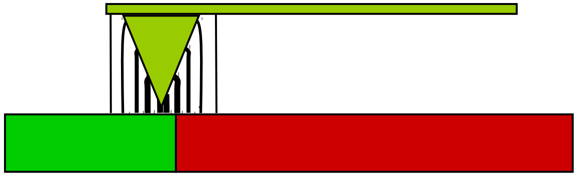

Experimental Setup
nc-AFM & AM-KPFM

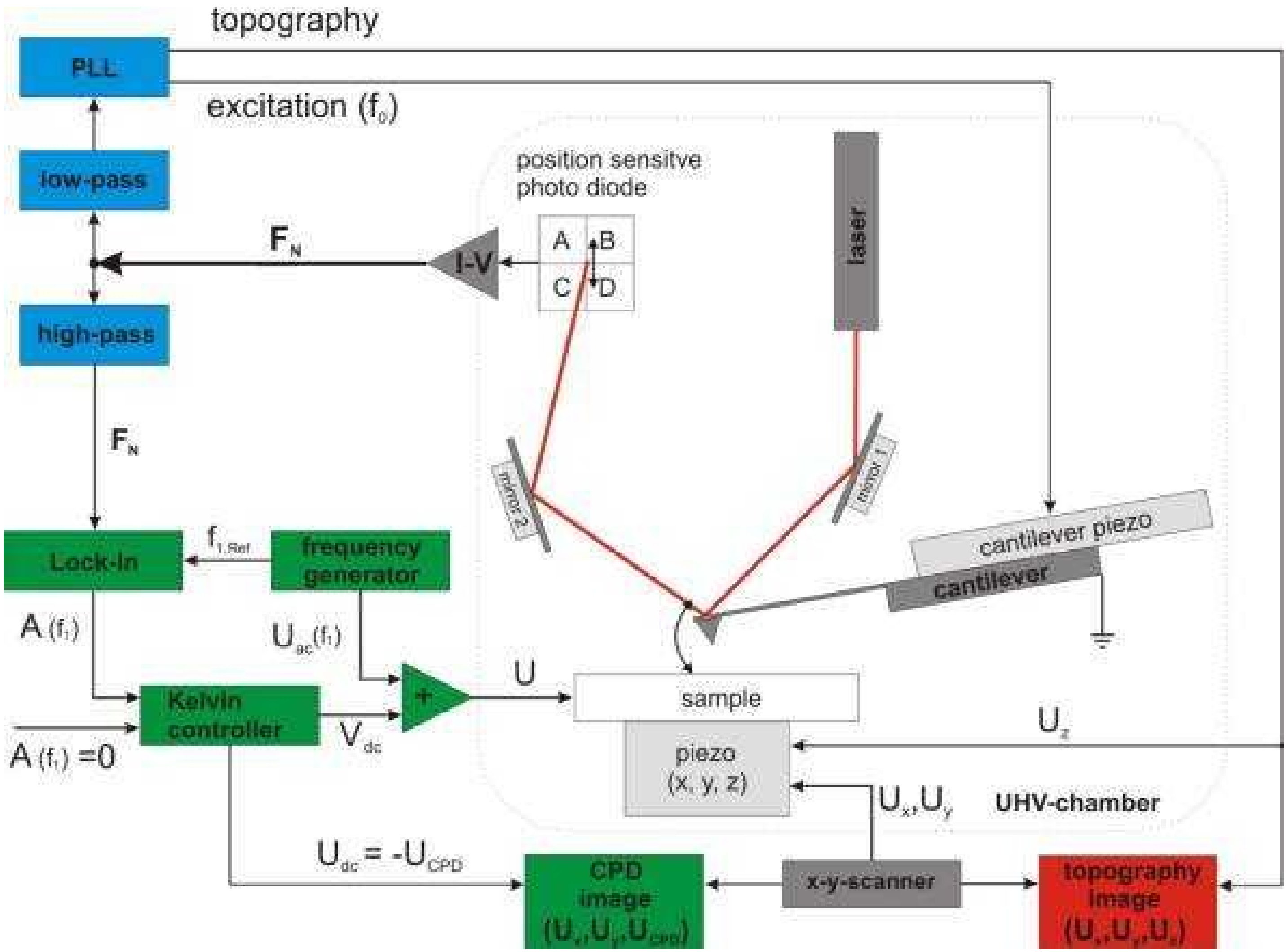

KPFM calibration and absolute work function

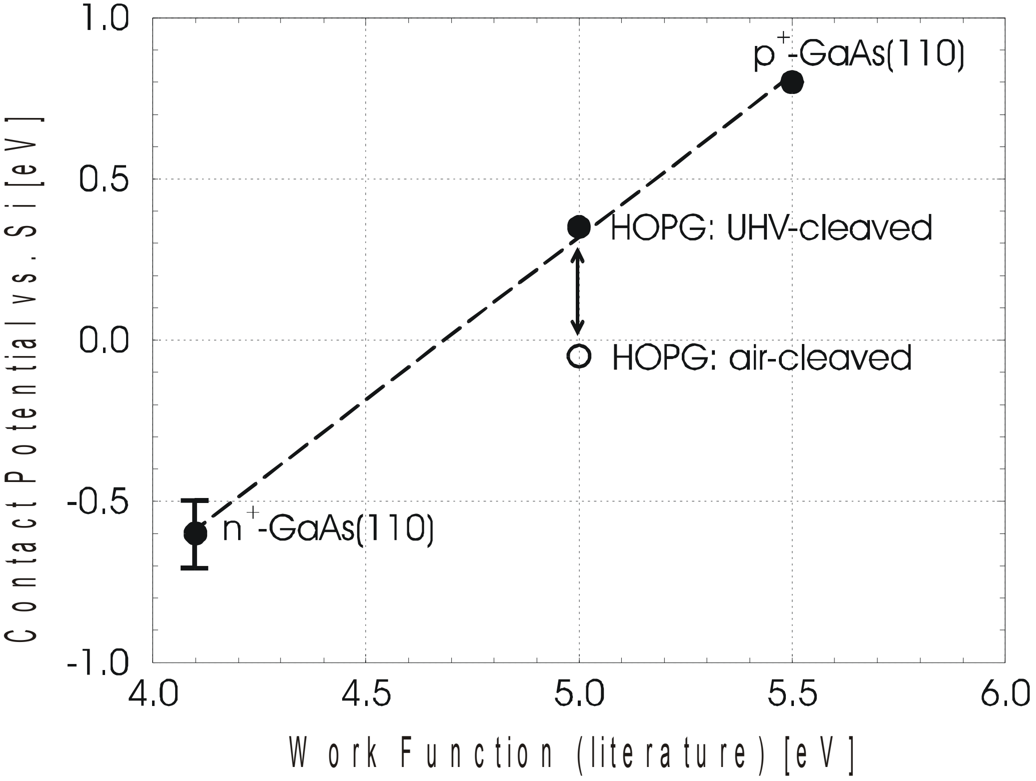

Φ-Si-Cantilever = 4.70 (±0.1) eV

U_{ac} = 100 mV

→ absolute and quantitative work function determination

Polished Cross Section of a $CuGaSe_2$ Solar Cell

$CuGaSe_2$ solar cell device: $V_{oc} = 820$ mV, $\eta = 4.6$ %

polished and Ar-ion sputtered cross section

topography work function

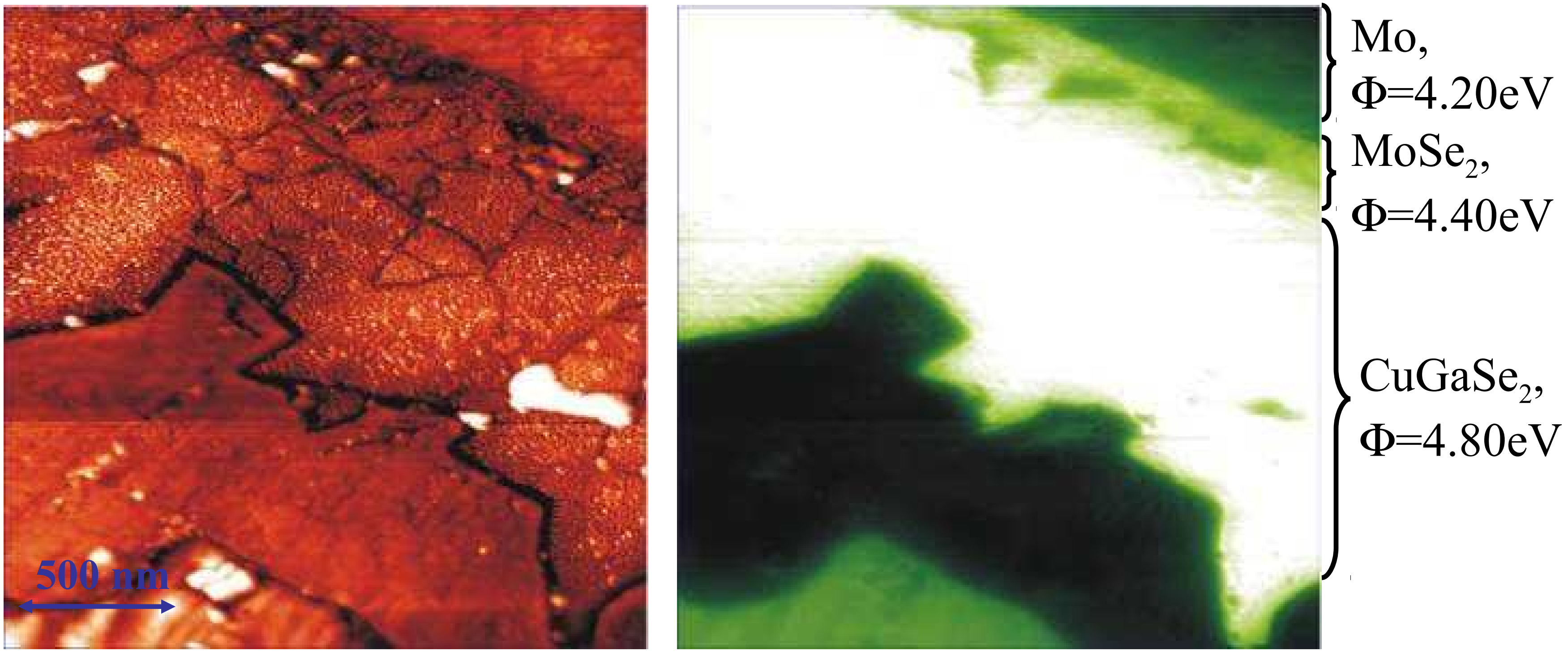

Δz = 65 nm

n-ZnO:Ga,
Φ=4.0eV

Glatzel *et al*., APL **81**, 2017 (2002)

Surface Photovoltage
MDMO-PPV/PCBM – 675nm

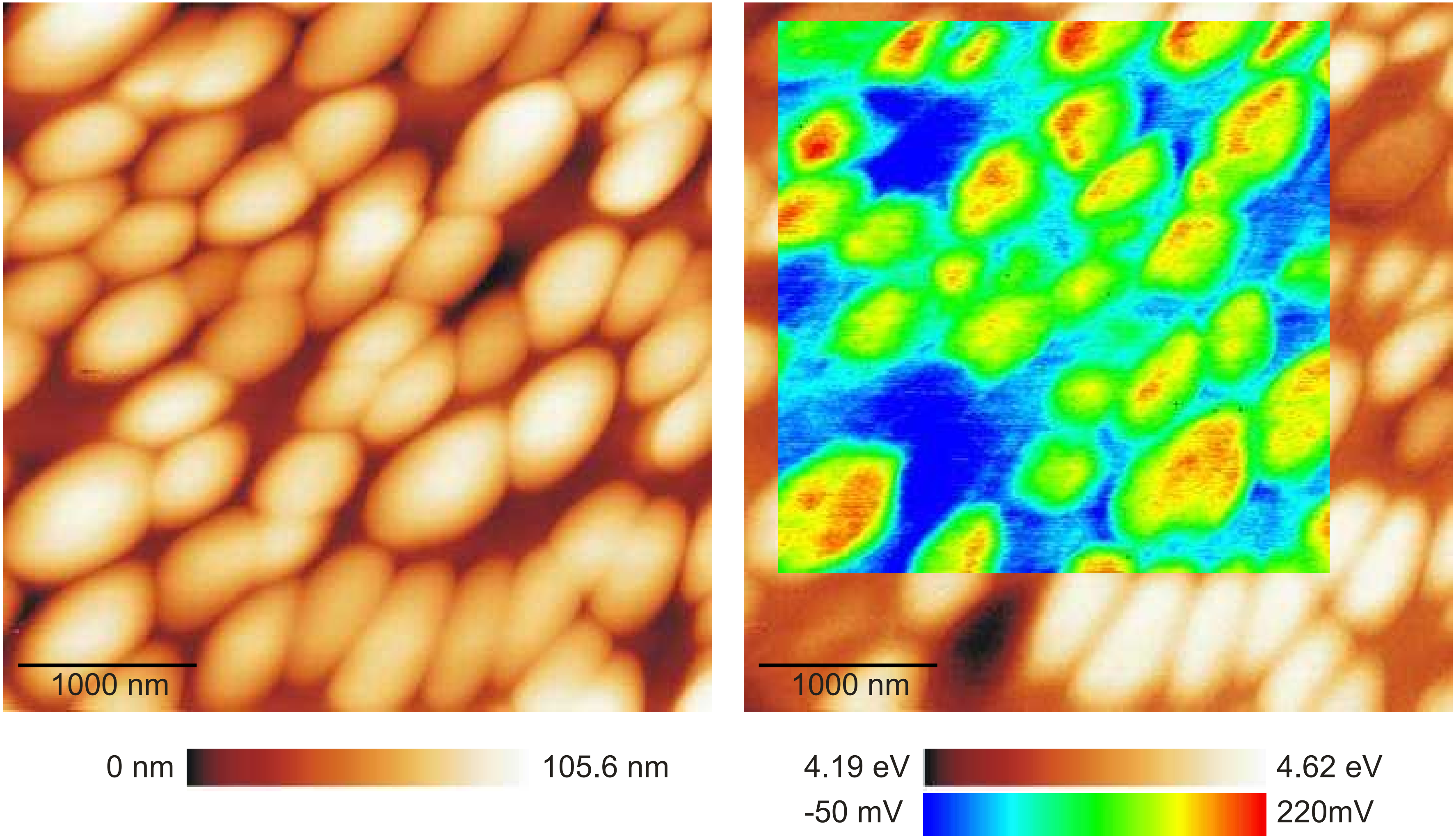

Functionalized Truxenes

Structure

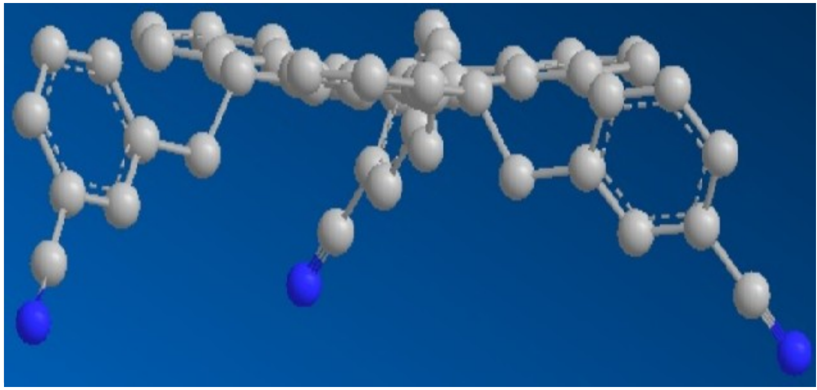

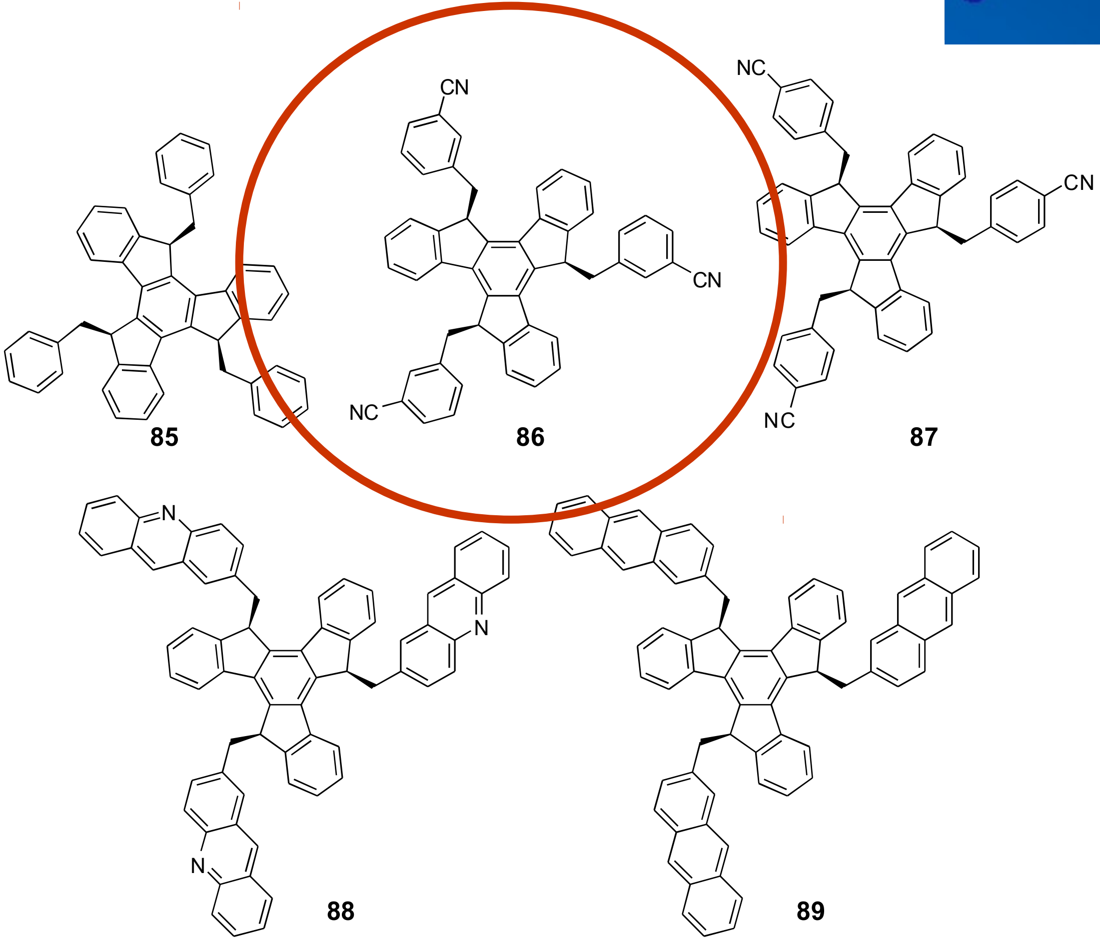

85

86

87

88

89

O. de Frutos et al., Chem. Eur. J. 8(13), 2879 (2002)

Single Crystal KBr

Substrate patterning by electron irradiation

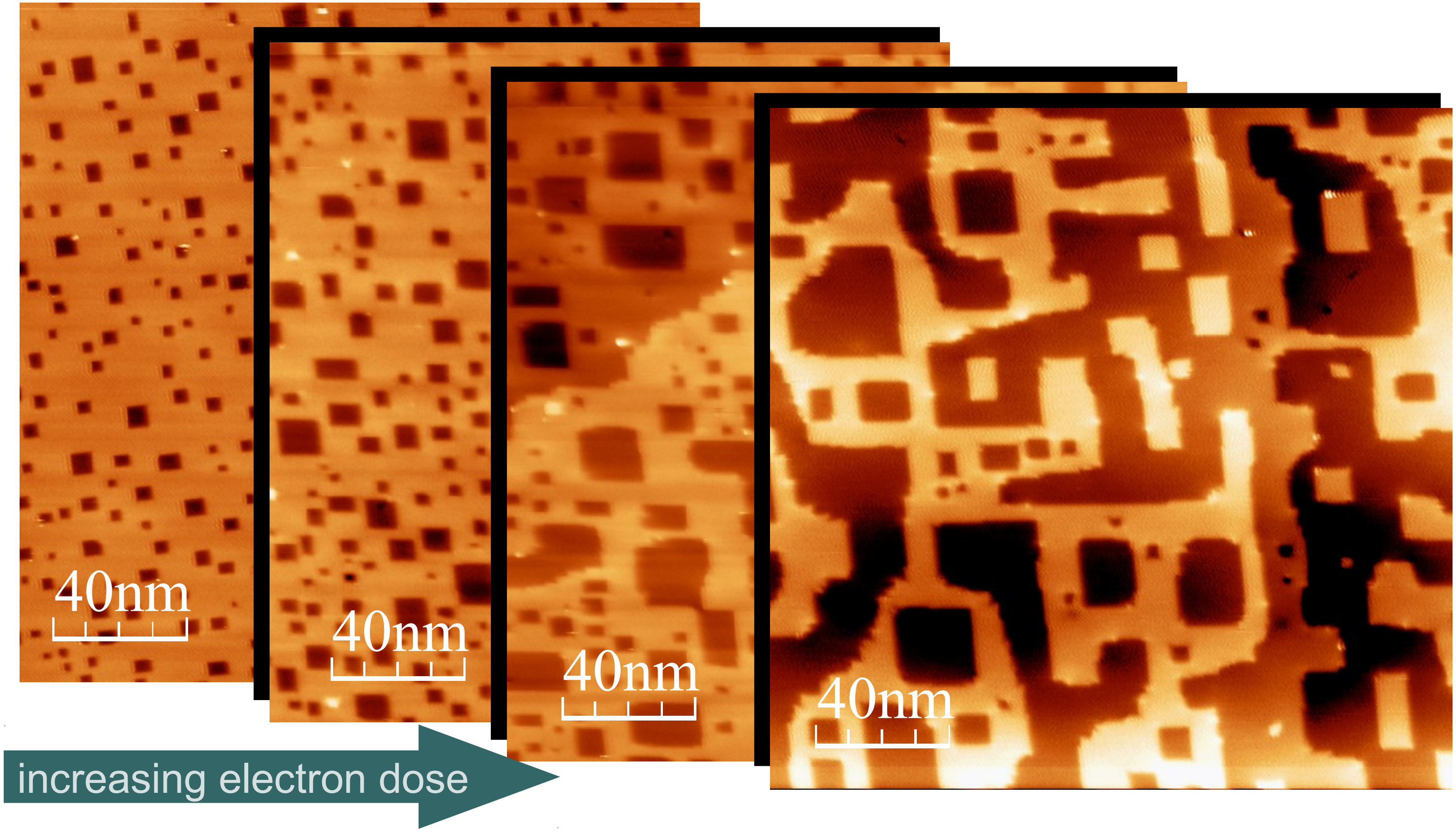

increasing electron dose

Truxenes on patterned surface

Filled and unfilled pits

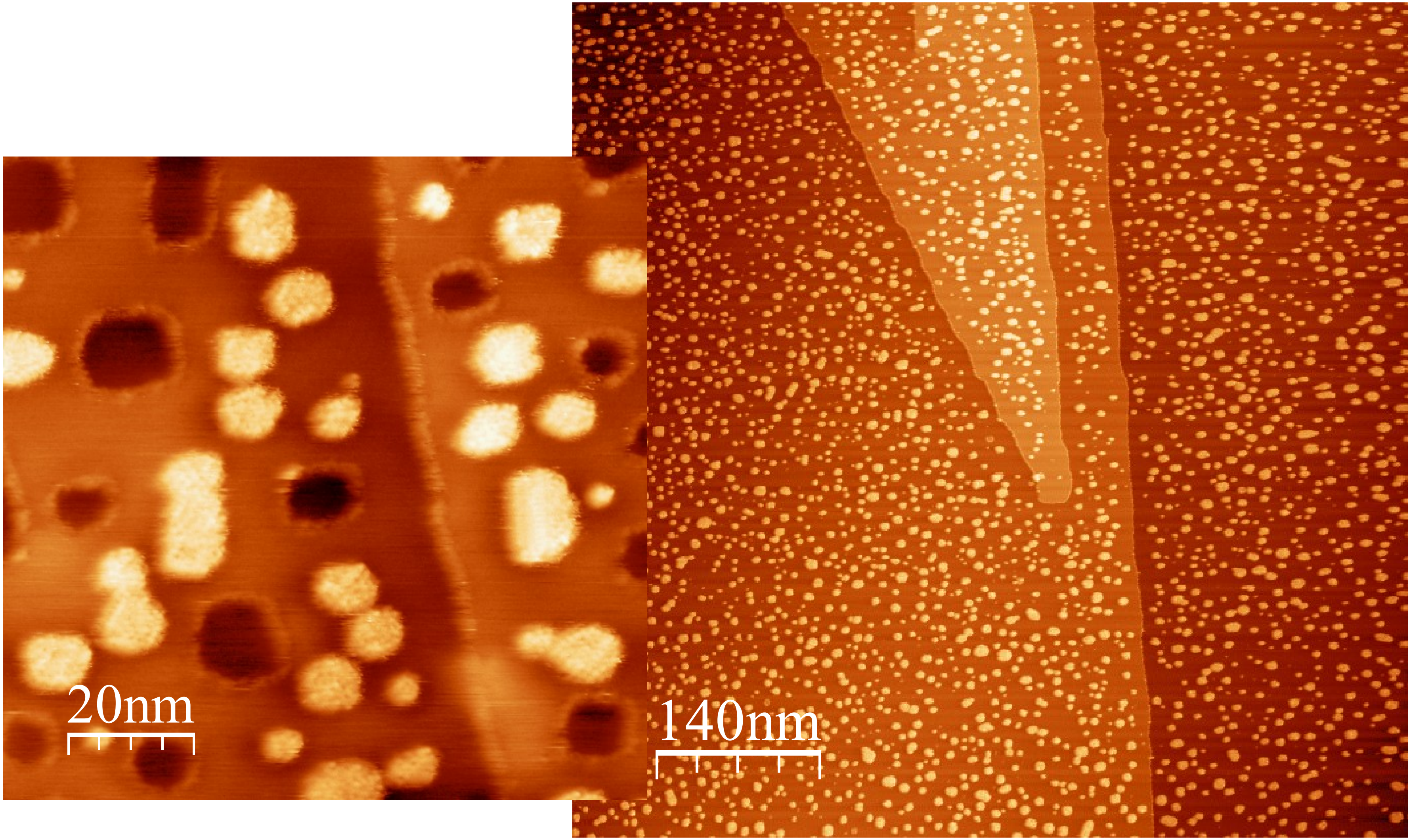

Truxenes on patterned surface

Organization within the pits

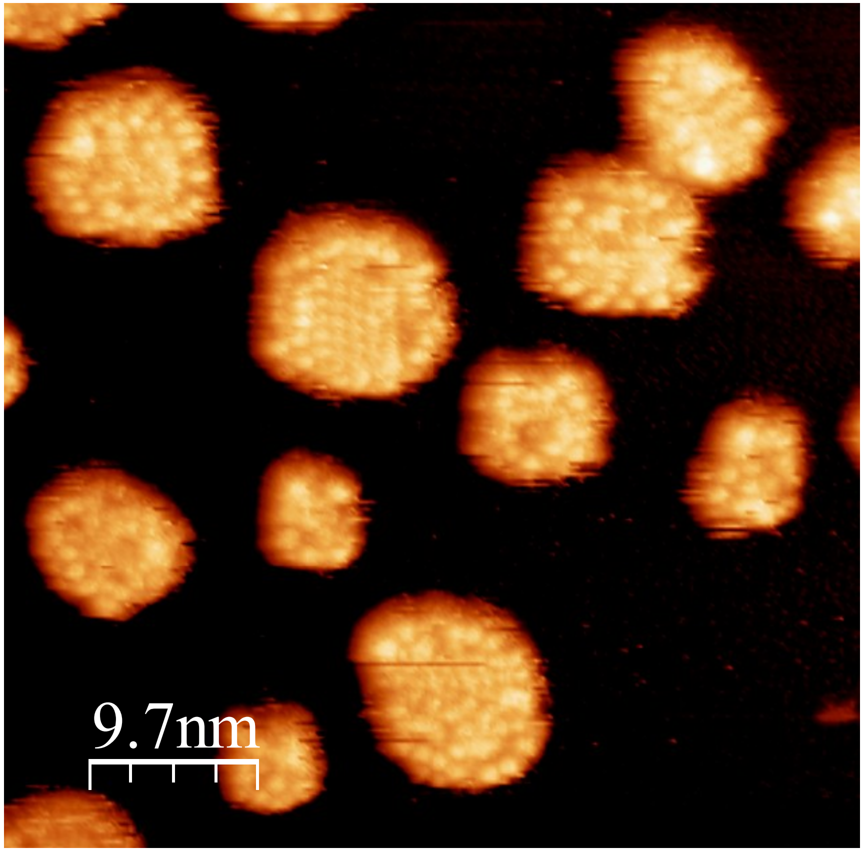

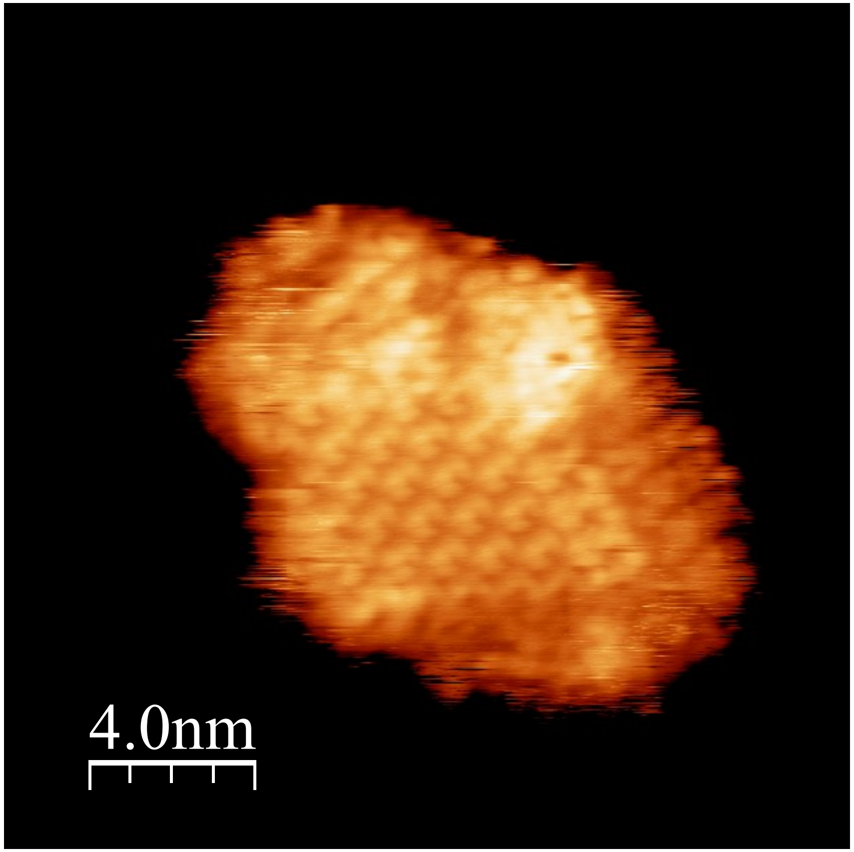

Imaging a Single Molecule

Measurements at RT

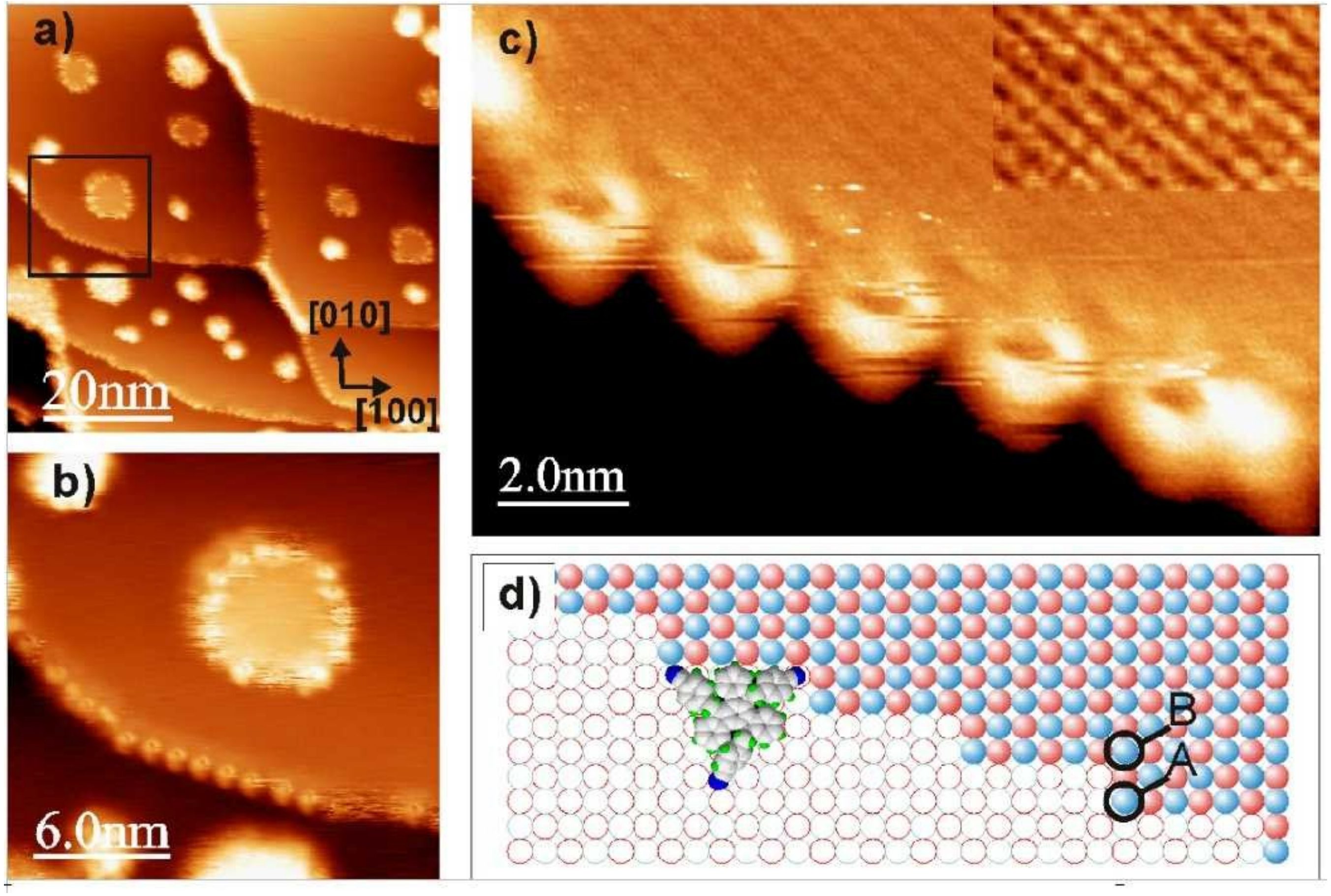

- Re-arrangement of the substrate, edges are running in the [-3 1 0] direction
- no chemical interaction with the surface
- adsorbed on K or Br terminated double atomic kink

Imaging a Single Molecule

Measurements at RT

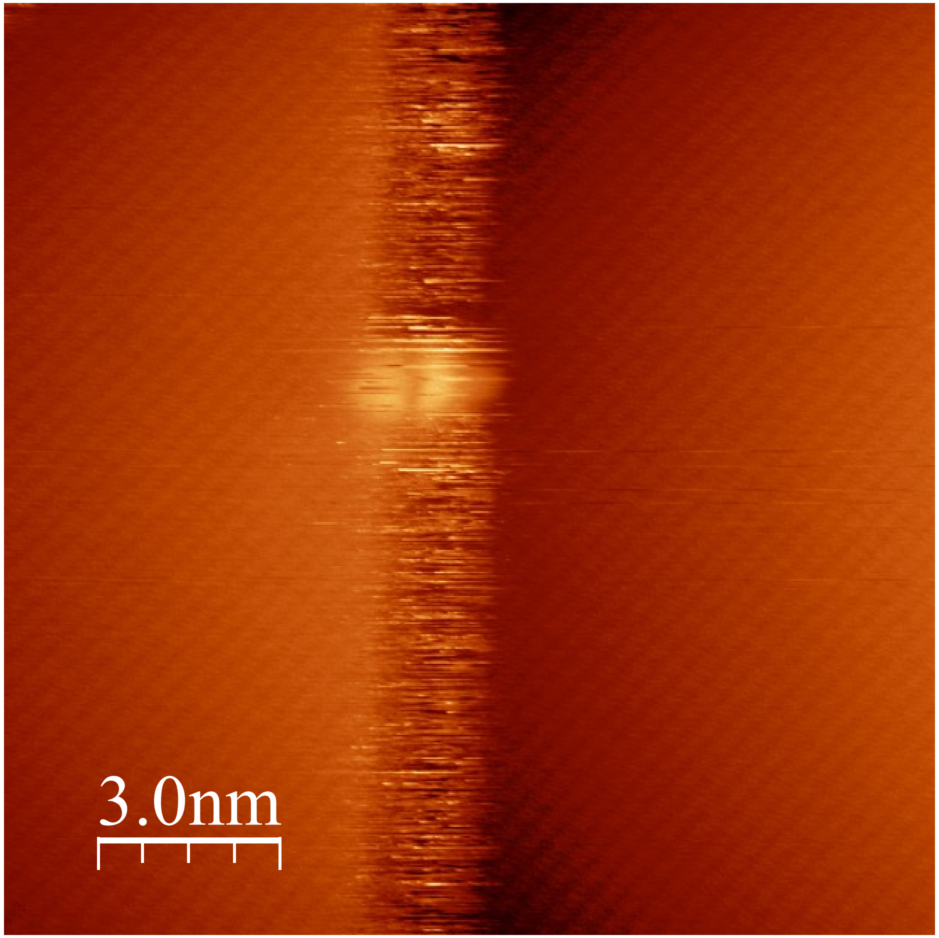

Br terminated, E_b=1.33eV

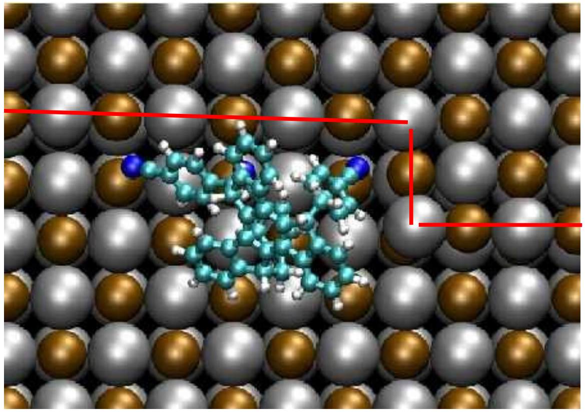

K terminated, E_b=1.17eV

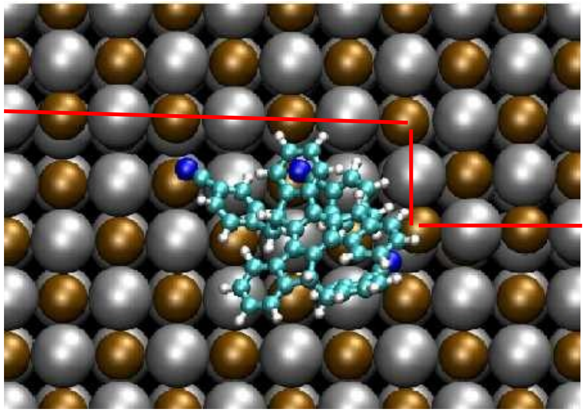

Porphyrin with bicyanophenyl legs

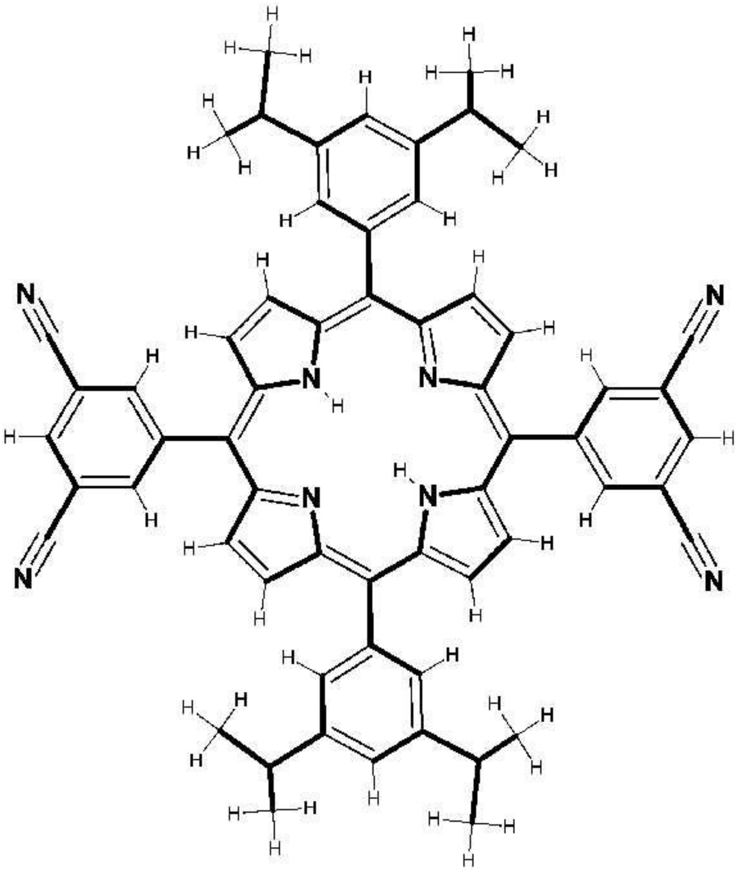

2-bicyanophenyl, 2-aryl H2-porphyrin
synthesized by F. Diederich (ETH, Zurich)

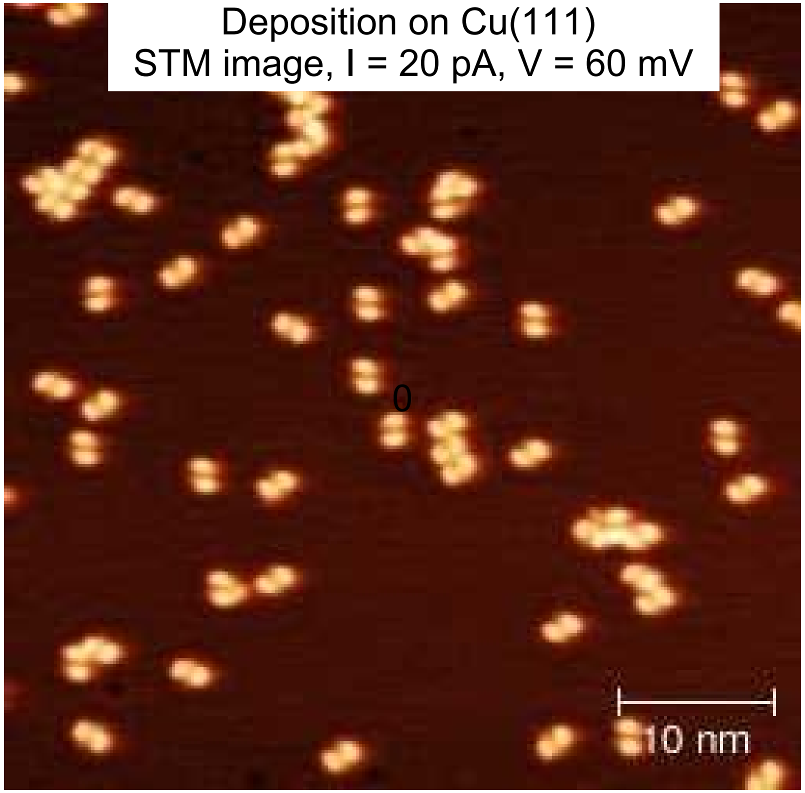
Deposition on Cu(111)
STM image, I = 20 pA, V = 60 mV

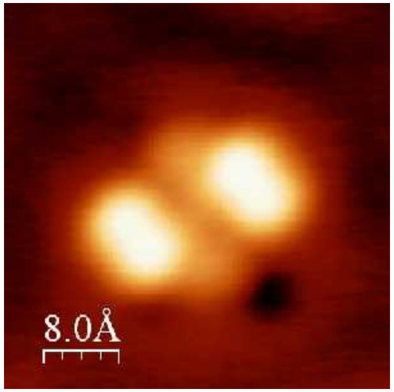

R. Pawlak et al.

Vertical manipulation: Catch the molecule…

Method: Z spectroscopic curve in the **center** of the molecule

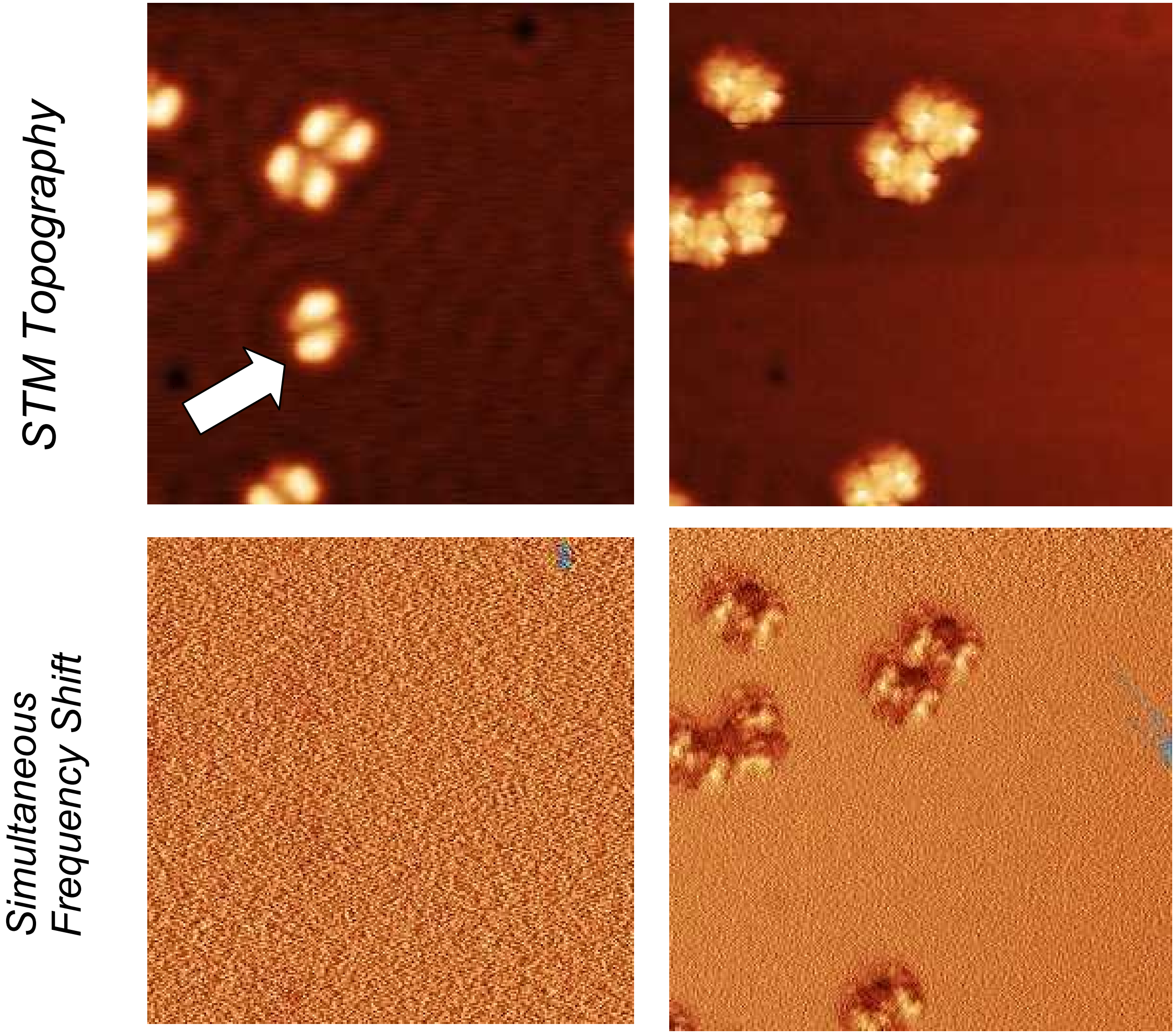

Friction measurement with a molecule linked to the tip

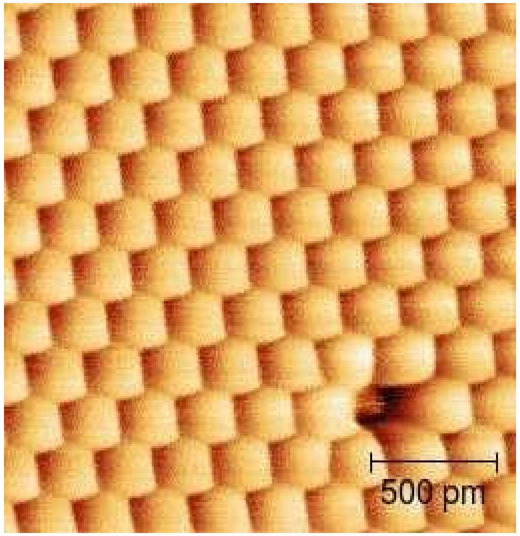

Atomic resolution on Cu(111)

3d-force spectroscopy: Observations of localized instabilities

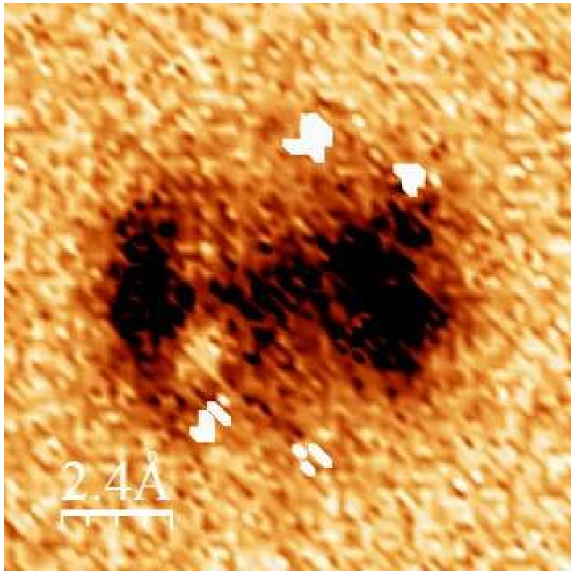

Three-dimensional
Force Field Spectroscopy

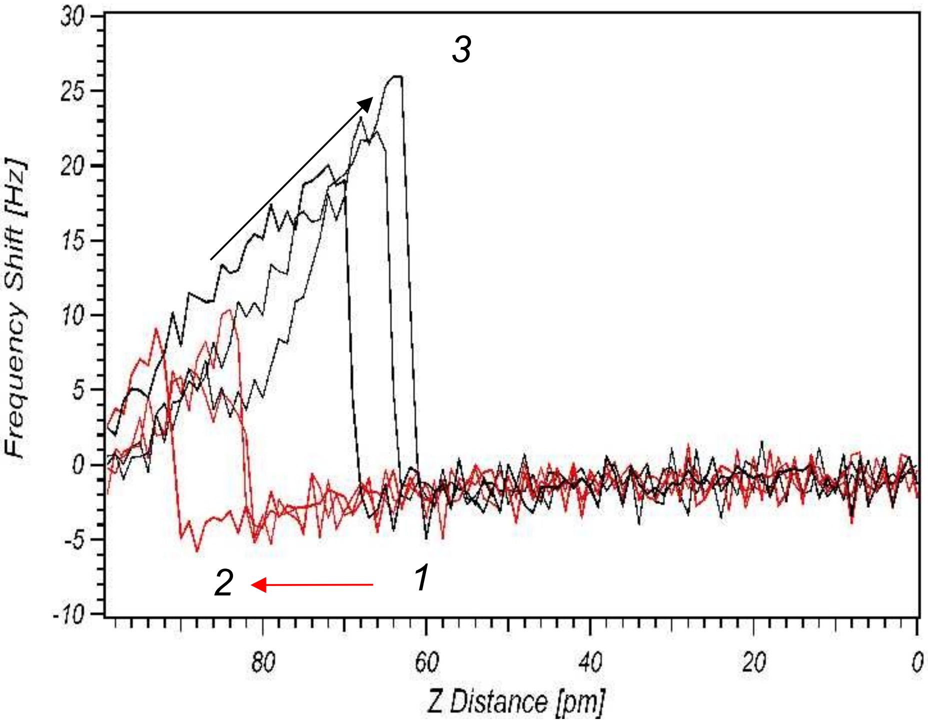

Origin of the hysteresis

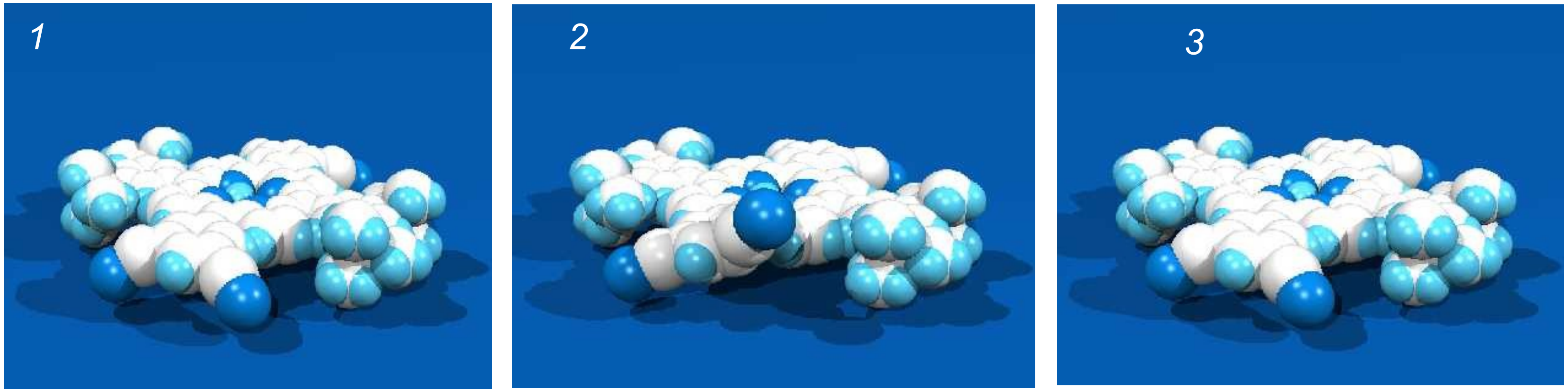

Vertical switching and statistics

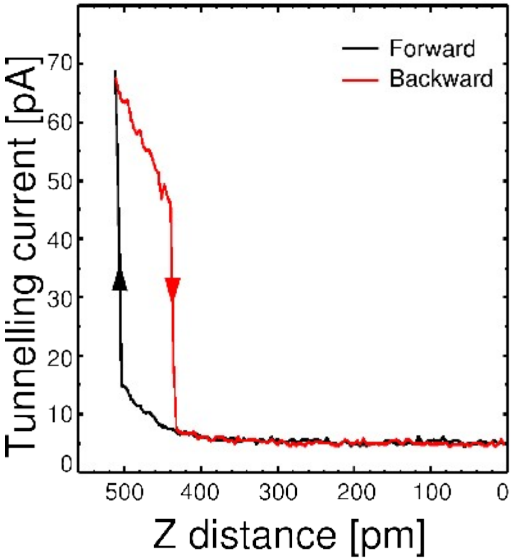

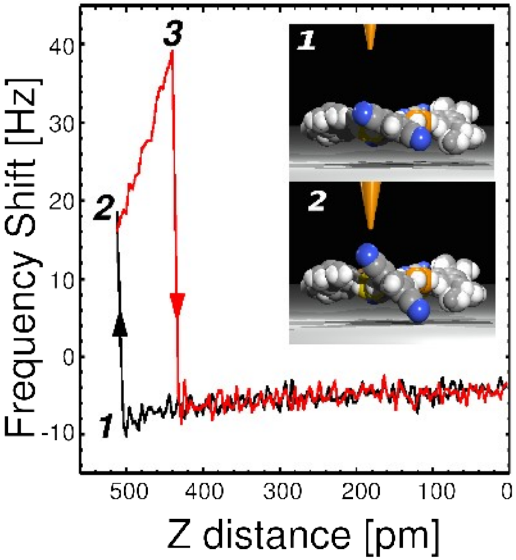

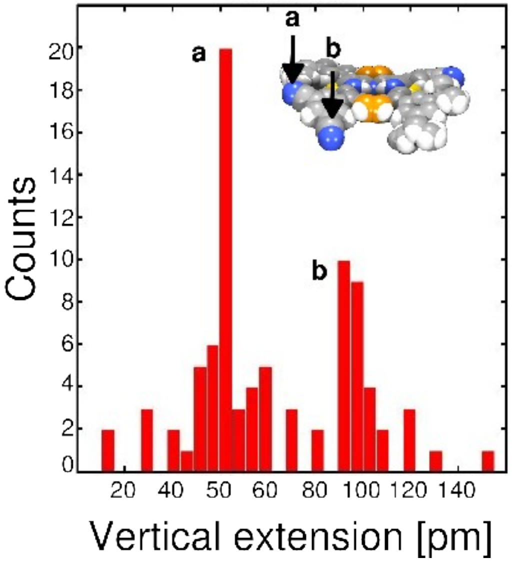

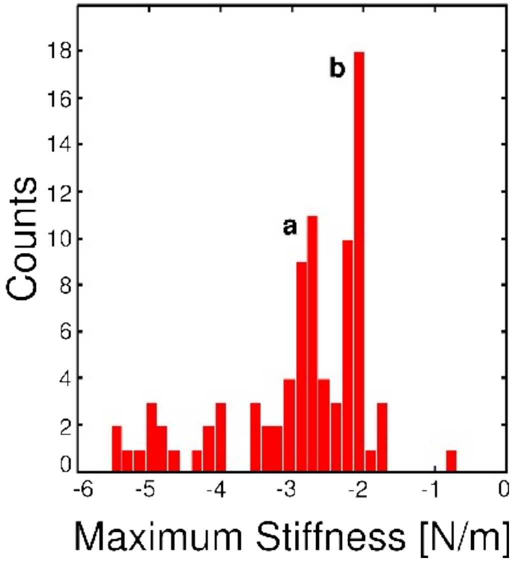

Vertical switching:

- **Tip-molecule junction between a CN function and the Cu-terminated tip.**
- **Attractive interaction force** *(= -150 pN)* **to create the bond.**
- **Possibility to lift the porphyrin leg up by retracting the tip.**
- *Elastic process* **independent of the targeted CN functions as well as the enantiomeric form.**

Rotation by controlled force interations

Rotational switching of the molecule:

- **Tip-induced motion of the porphyrin by manipulating the CN function with a single *z* spectroscopic curve.**
- **Rotation of 60° with respect to the initial conformation.**
- **Absolute interaction force =** - 500 pN **during manipulation, dissipated energy =** 30-80 meV/cycle**.**
- Fully elastic process **(no tunnelling current and bias variation).**

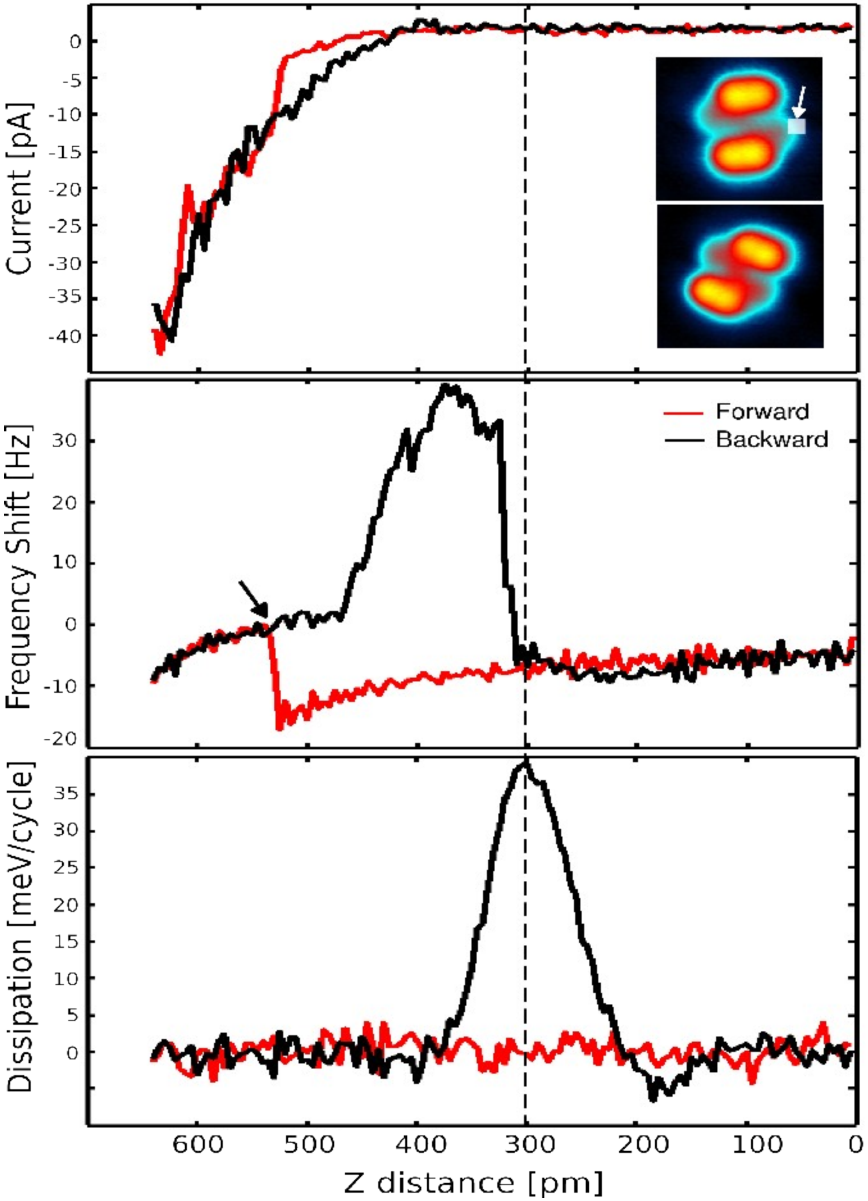

Rotation of molecules clockwise and anticlockwise

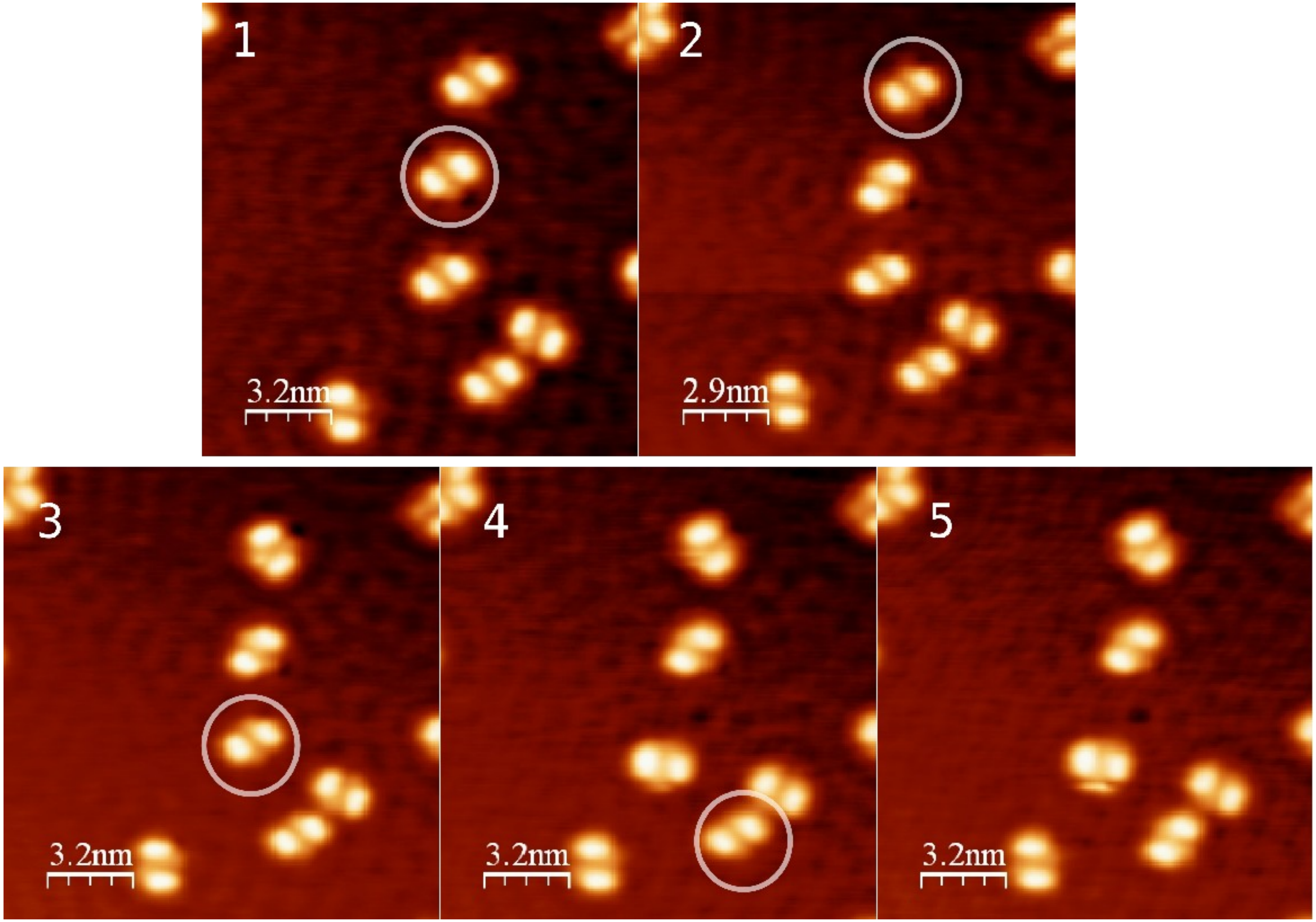

- Possibility to rotate molecules in both directions (clockwise and anticlockwise) without consideration to their symmetry

nc-AFM Messungen

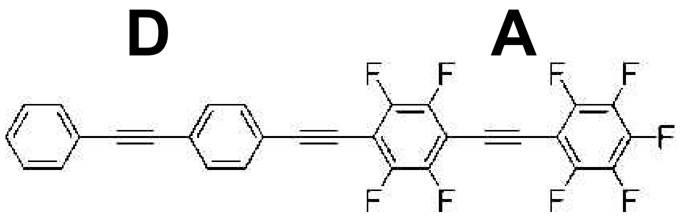

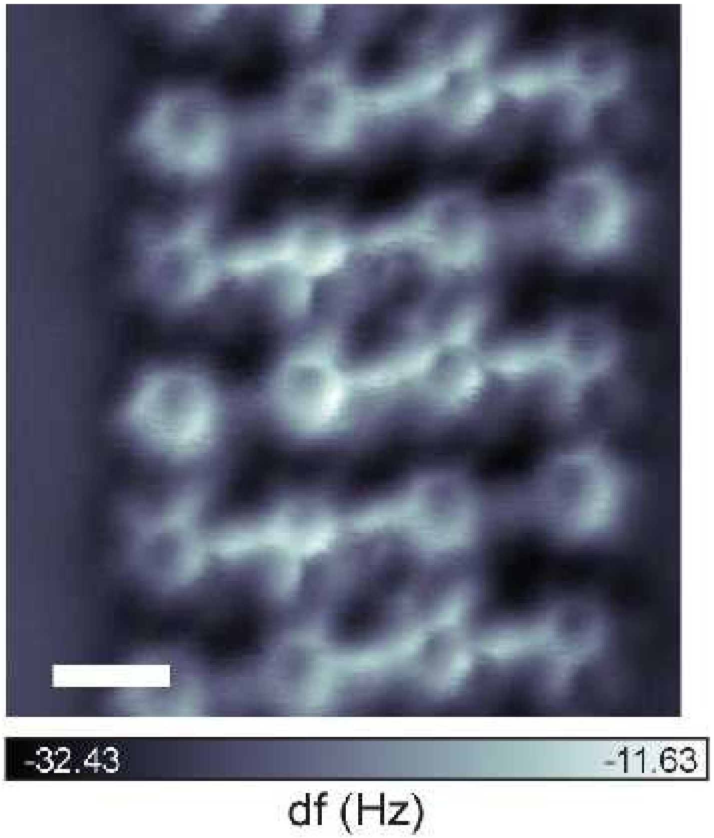

DA molecules on

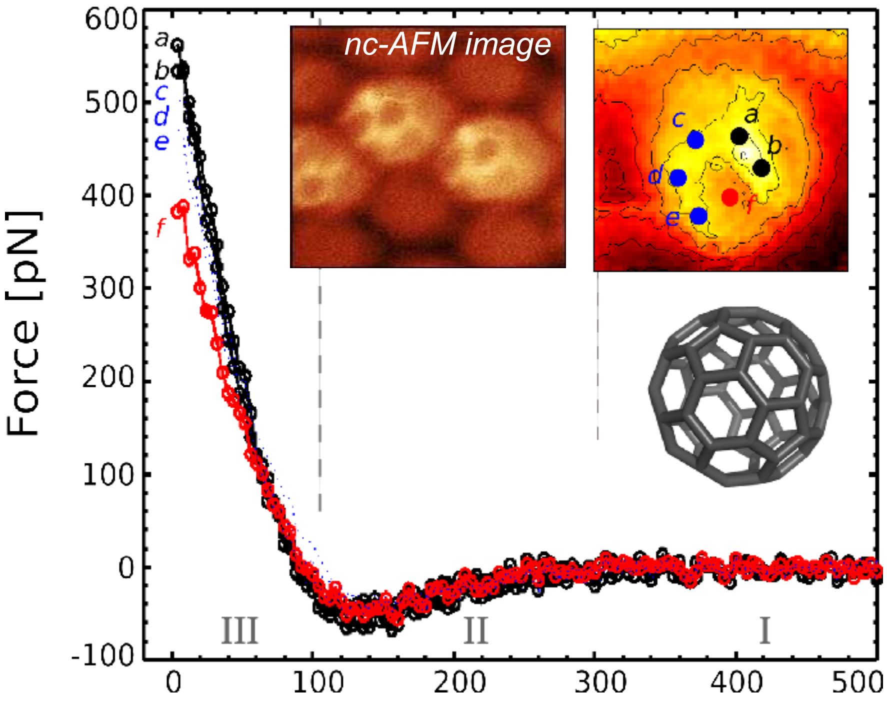

C$_{60}$ on Cu(111), Kraftspektroskopie

A Small Swiss Cross made by AFM at room temperature torsional resonance imaging

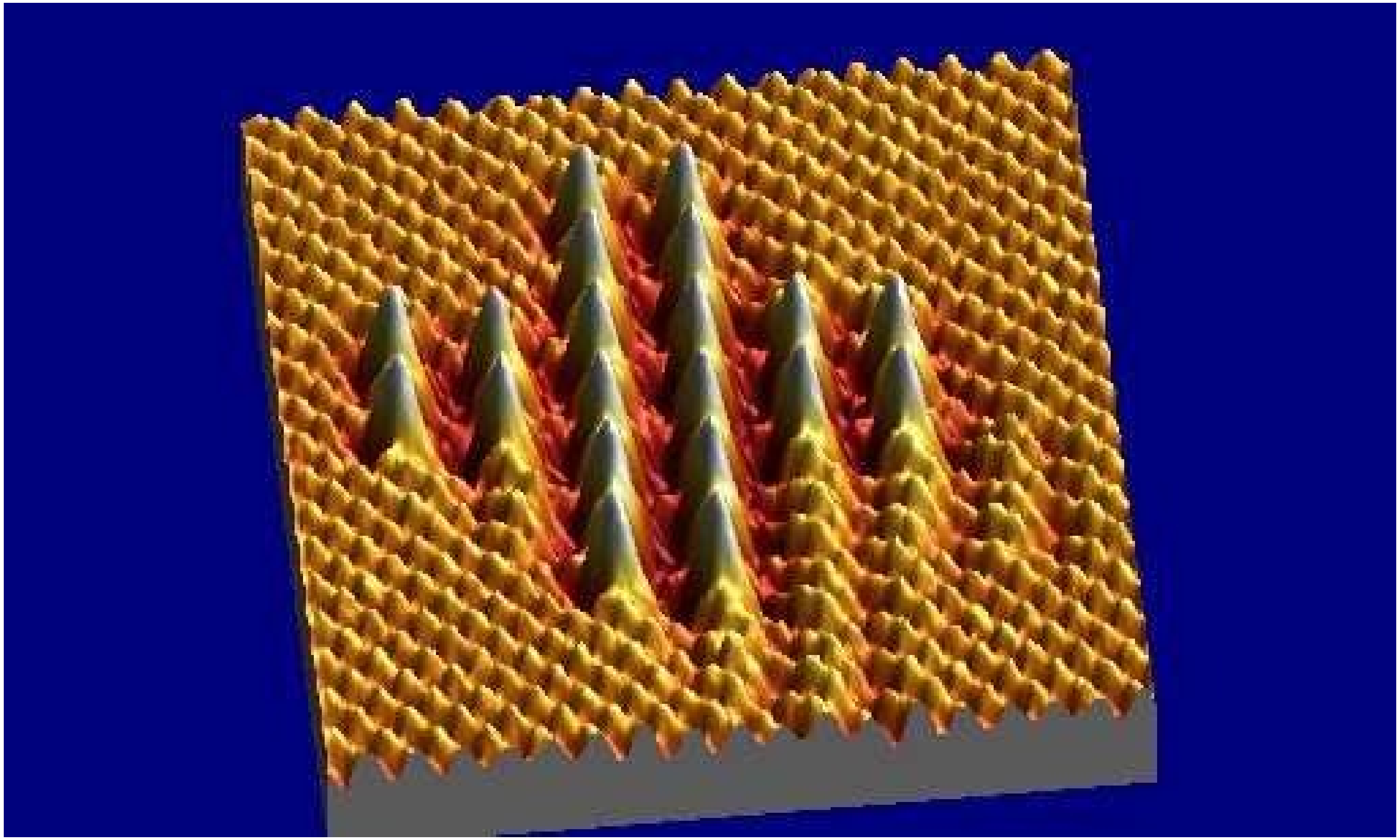

S. Shigeki et al.

Nanostrukturen-Analysemethoden

Secondary Ion Mass Spectrometry (SIMS)

Principles, Instrumentation, Applications

- **Principles**
- **Instrumentation**
- **Applications**
    - Depth profiling
    - 2D imaging
    - 3D imaging

Thilo Glatzel, thilo.glatzel@unibas.ch
NANOlino Lab

Centre de Recherche Public Gabriel Lippmann

based on slides from ***T. Wirtz, CRP-Gabriel Lippmann, Luxembourg***

Joseph John Thomson
(1856 – 1940)

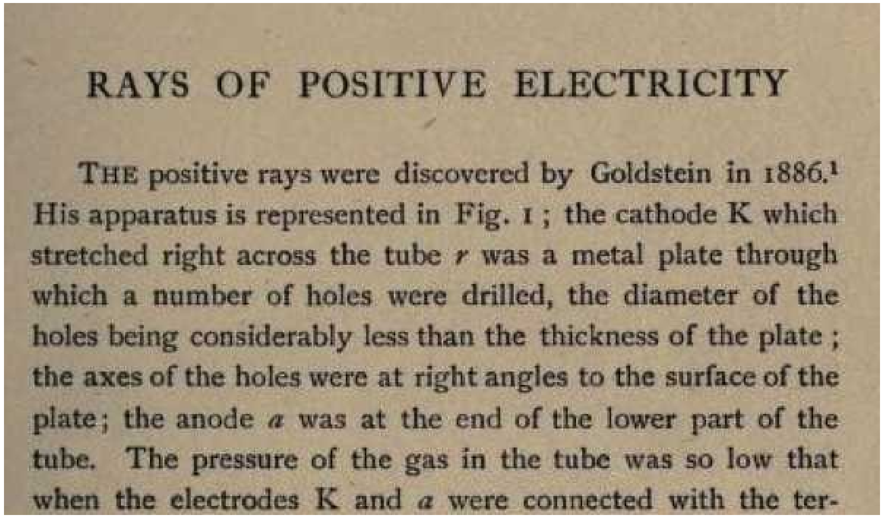

RAYS OF POSITIVE ELECTRICITY

THE positive rays were discovered by Goldstein in 1886.[1] His apparatus is represented in Fig. 1; the cathode K which stretched right across the tube *r* was a metal plate through which a number of holes were drilled, the diameter of the holes being considerably less than the thickness of the plate; the axes of the holes were at right angles to the surface of the plate; the anode *a* was at the end of the lower part of the tube. The pressure of the gas in the tube was so low that when the electrodes K and *a* were connected with the ter-

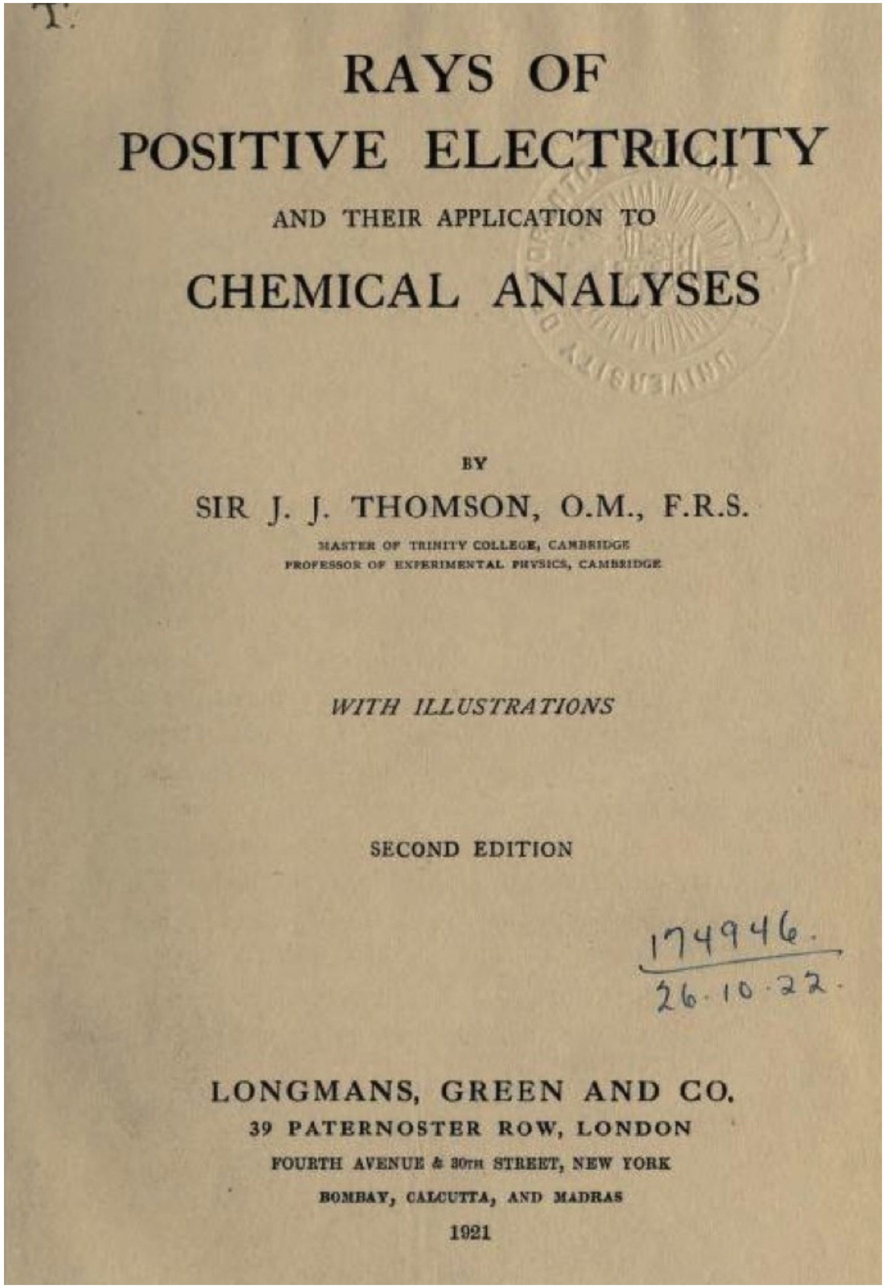

RAYS OF
POSITIVE ELECTRICITY
AND THEIR APPLICATION TO
CHEMICAL ANALYSES

BY
SIR J. J. THOMSON, O.M., F.R.S.
MASTER OF TRINITY COLLEGE, CAMBRIDGE
PROFESSOR OF EXPERIMENTAL PHYSICS, CAMBRIDGE

WITH ILLUSTRATIONS

SECOND EDITION

LONGMANS, GREEN AND CO.
39 PATERNOSTER ROW, LONDON
FOURTH AVENUE & 30TH STREET, NEW YORK
BOMBAY, CALCUTTA, AND MADRAS
1921

Principles

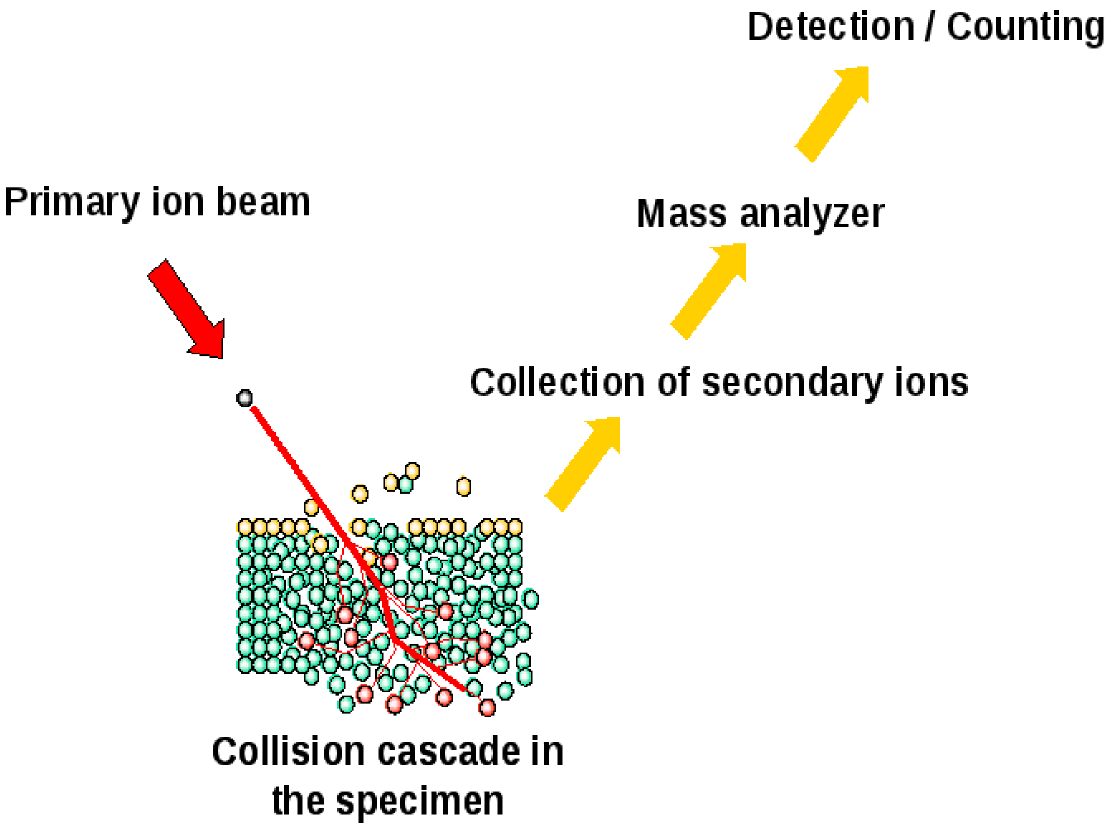

Detection / Counting

Primary ion beam

Mass analyzer

Collection of secondary ions

Collision cascade in the specimen

SIMS is a surface analysis technique used to characterize the **surface and sub-surface region** of materials. It effectively employs the **mass spectrometry of ionised particles** which are emitted when a surface, normally a solid, is bombarded by energetic primary particles. The **primary particles may be electrons, ions, neutrals or photons**.

Principles

Ion Beam Sputtering

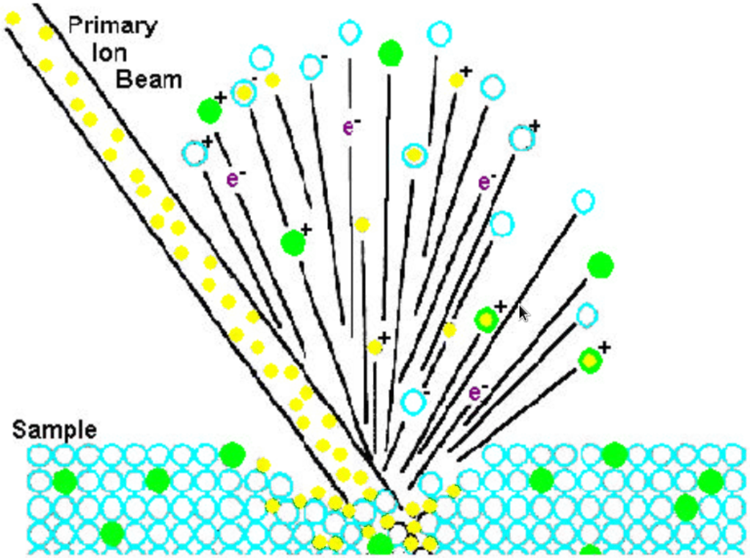

The bombarding primary ion beam produces **monatomic and polyatomic particles of sample material** and **resputtered primary ions**, along with **electrons and photons**. The secondary particles carry negative, positive, and neutral charges and they have **kinetic energies that range from zero to several hundred eV**.

Primary beam species useful in SIMS include Cs^+, O_2^+, O , Ar^+, and Ga^+ at energies between 1 and 30keV. Primary ions are **implanted and mix with sample** atoms to depths of 1 to 10nm. **Sputter rates** in typical SIMS experiments vary between **0.5 and 5nm/s**. Sputter rates depend on primary beam intensity, sample material, and crystal orientation.
The sputter yield is the ratio of the number of atoms sputtered to the number of impinging primary ions. Typical SIMS sputter yields fall in a range from 5 and 15.

Principles

Sputtering Effects

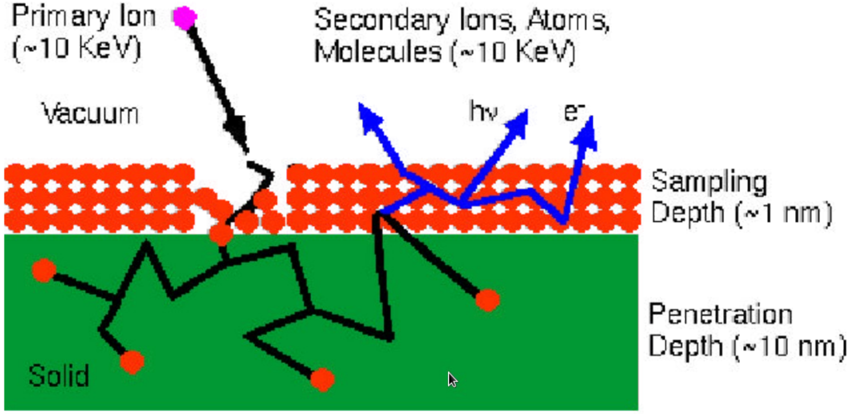

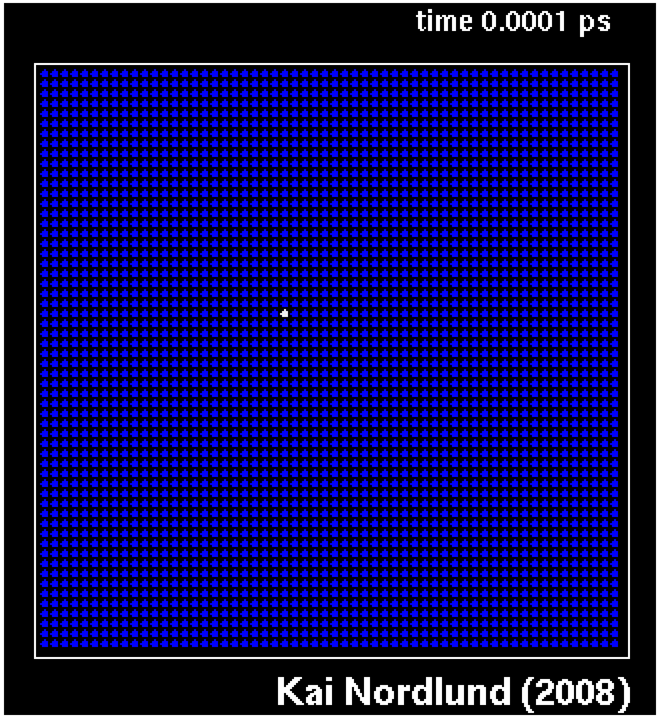

Sputtering leads to **surface roughness in the sputter craters**. **Lattice imperfections**, either already present or introduced by surface mixing, can be germs for roughness that takes the form of ribbons, furrows, ridges, cones, and agglomerations of cones. Polycrystalline materials form rough crater bottoms because of differential **sputter rates that depend on crystal orientation**.

The **collision cascade model** has the best success at quantitatively explaining how the **primary beam interacts with the sample atoms.** In this model, a fast primary ion passes energy to target atoms in a series of binary collisions. Energetic target atoms (called **recoil atoms**) collide with more target atoms. Target atoms that recoil back through the sample surface constitute sputtered material.
Atoms from the sample's outer monolayer can be driven in about 10 nm, thus **producing surface mixing**.

Principle

Secondary ion intensity: $I(M^{+/-}) \approx I_p \times Y_M \times c_M \times \beta_M^{+/-} \times T$

I_p: primary ion current
Y_M: partial sputtering yield of the element M
c_M: concentration of the element M
$\beta_M^{+/-}$: positive/negative ionisation probability of the emitted atom M
T: Instrumental transmission function

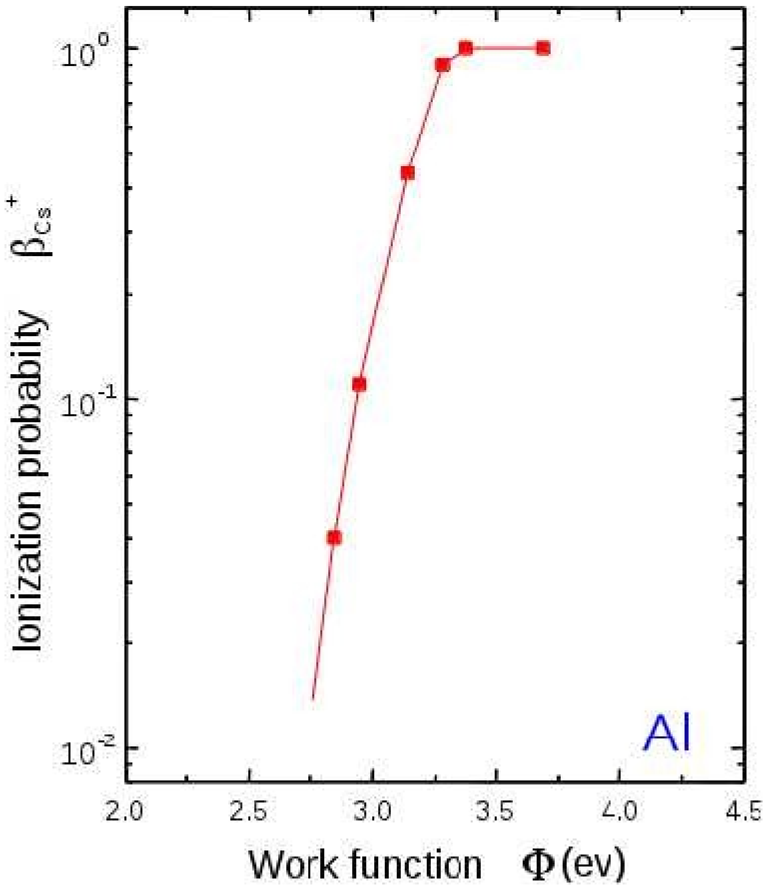

Different models for ion formation:

- electron tunneling model
- bond breaking model
- …

► difficult to predict $\beta_M^{+/-}$
(variation over several orders of magnitude)

Principles

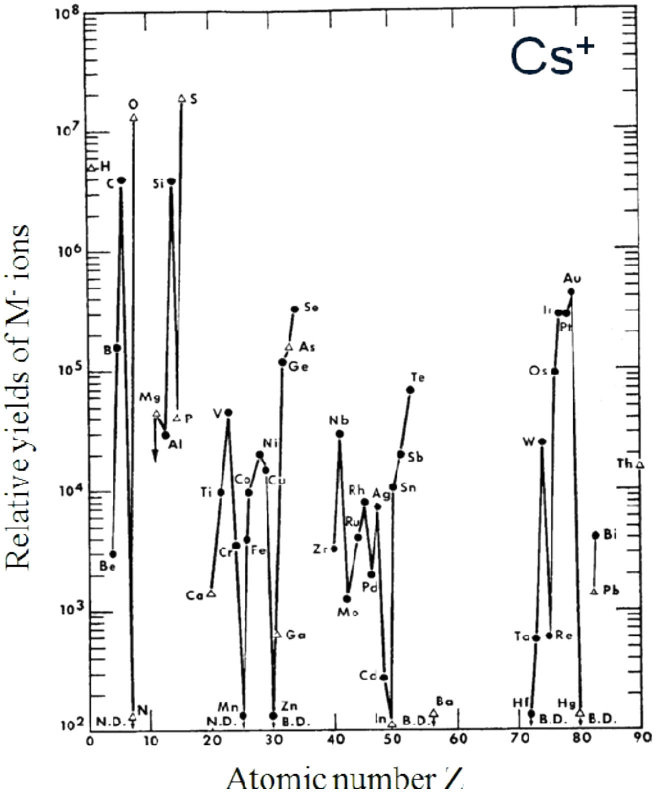

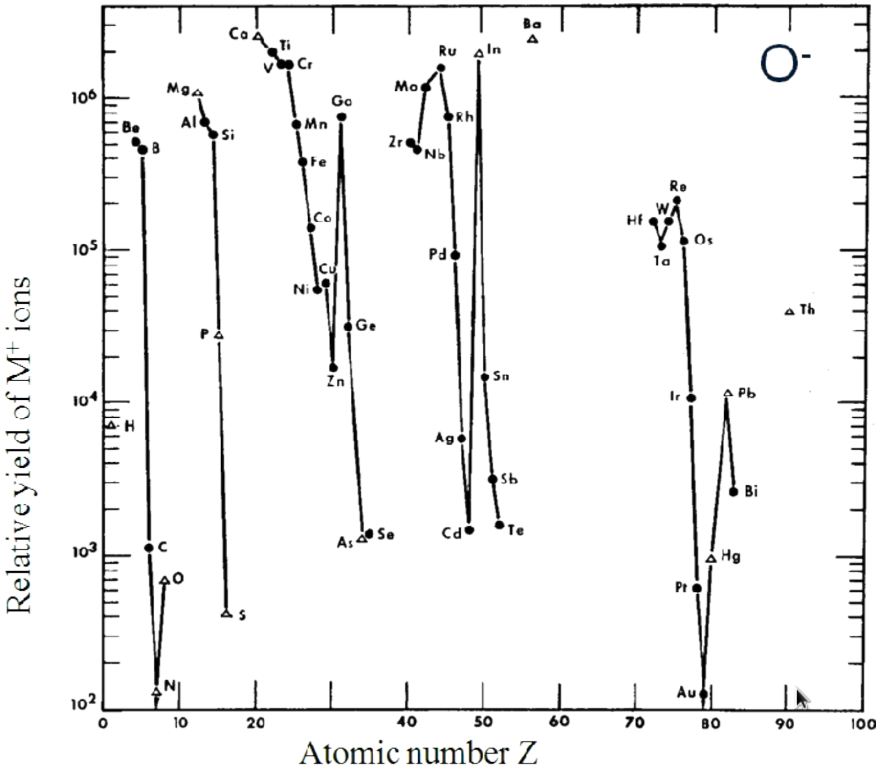

The emission of secondary ions is very sensitive to the chemical state of the sample surface:

- electro-positive primary ions (e.g. Cs^+) > increase of negative secondary ion emission (lower work function due to Cs)
- electro-negative primary ions (e.g. O_2^+ or O^-) > increase of positive secondary ion emission (high electron affinity of O)

Principles

Matrix-effect

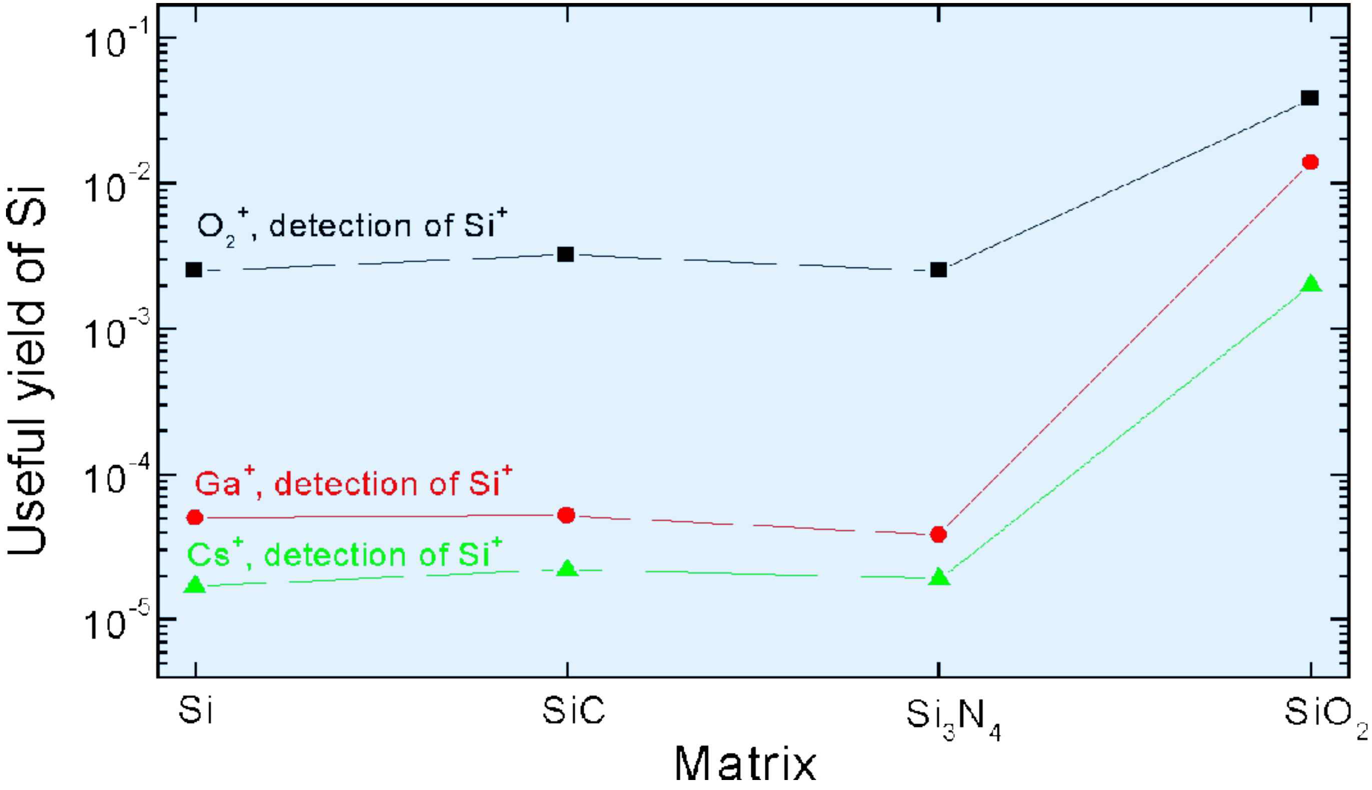

The ionization probability depends on the sample composition
Problems when interpreting and quantifying the results

Principles

Quantification – MCs_x^+ technique

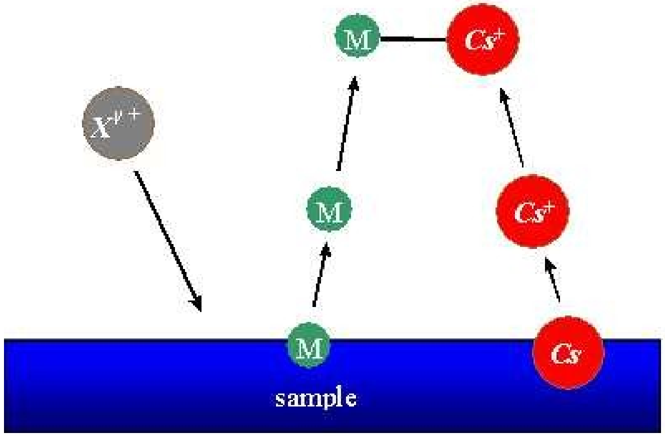

$$M^0 + Cs^+ \rightarrow MCs^+$$

$$\left\{ \begin{array}{l} M^0 + Cs_2^+ \rightarrow MCs_2^+ \\ MCs^0 + Cs^+ \rightarrow MCs_2^+ \\ M^- + Cs^+ + Cs^+ \rightarrow MCs_2^+ \end{array} \right.$$

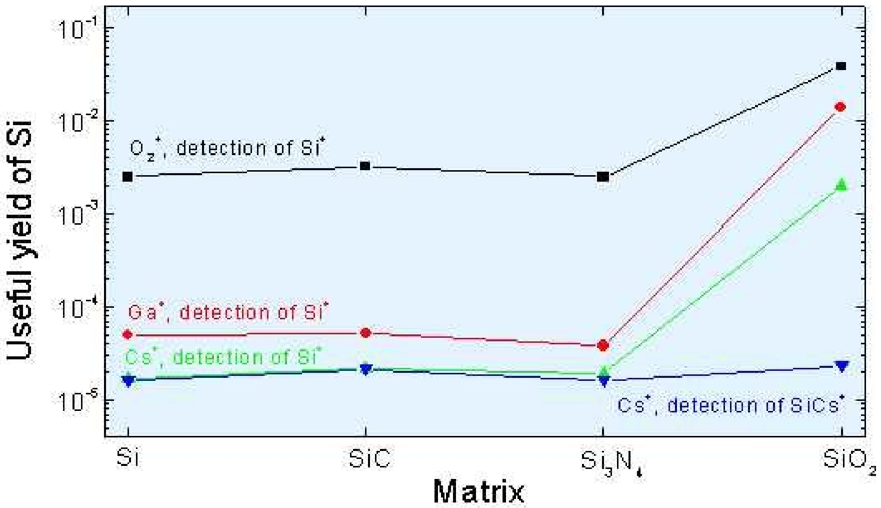

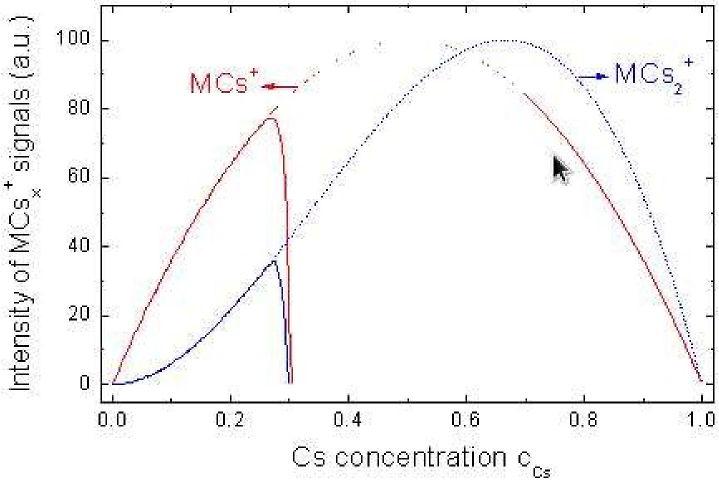

Instrumentation

Spectrometers

Dynamic SIMS

Static SIMS

Magnetic sector

Quadrupole

Time-of-Flight

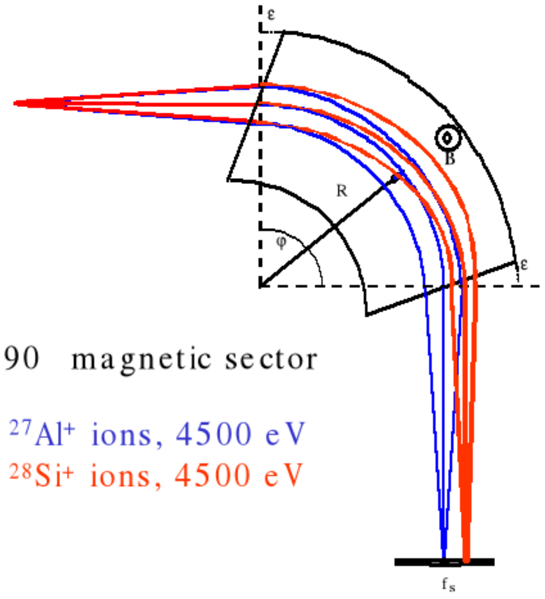

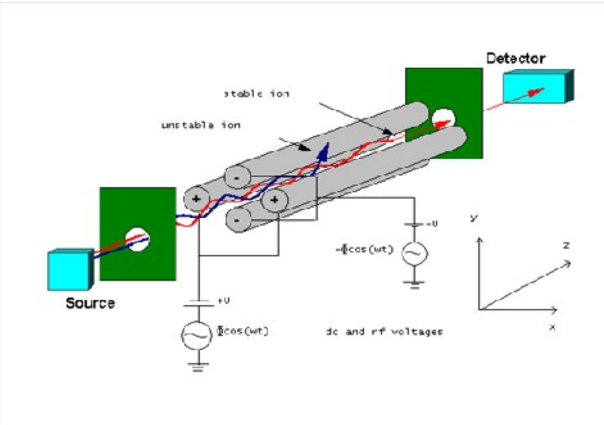

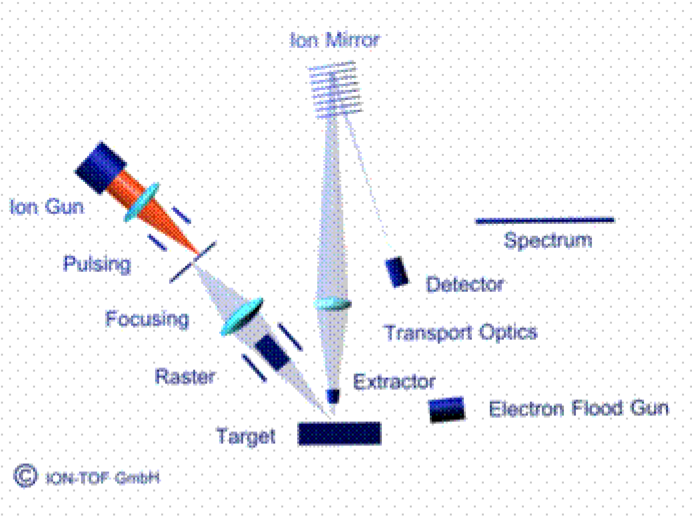

Instrumentation

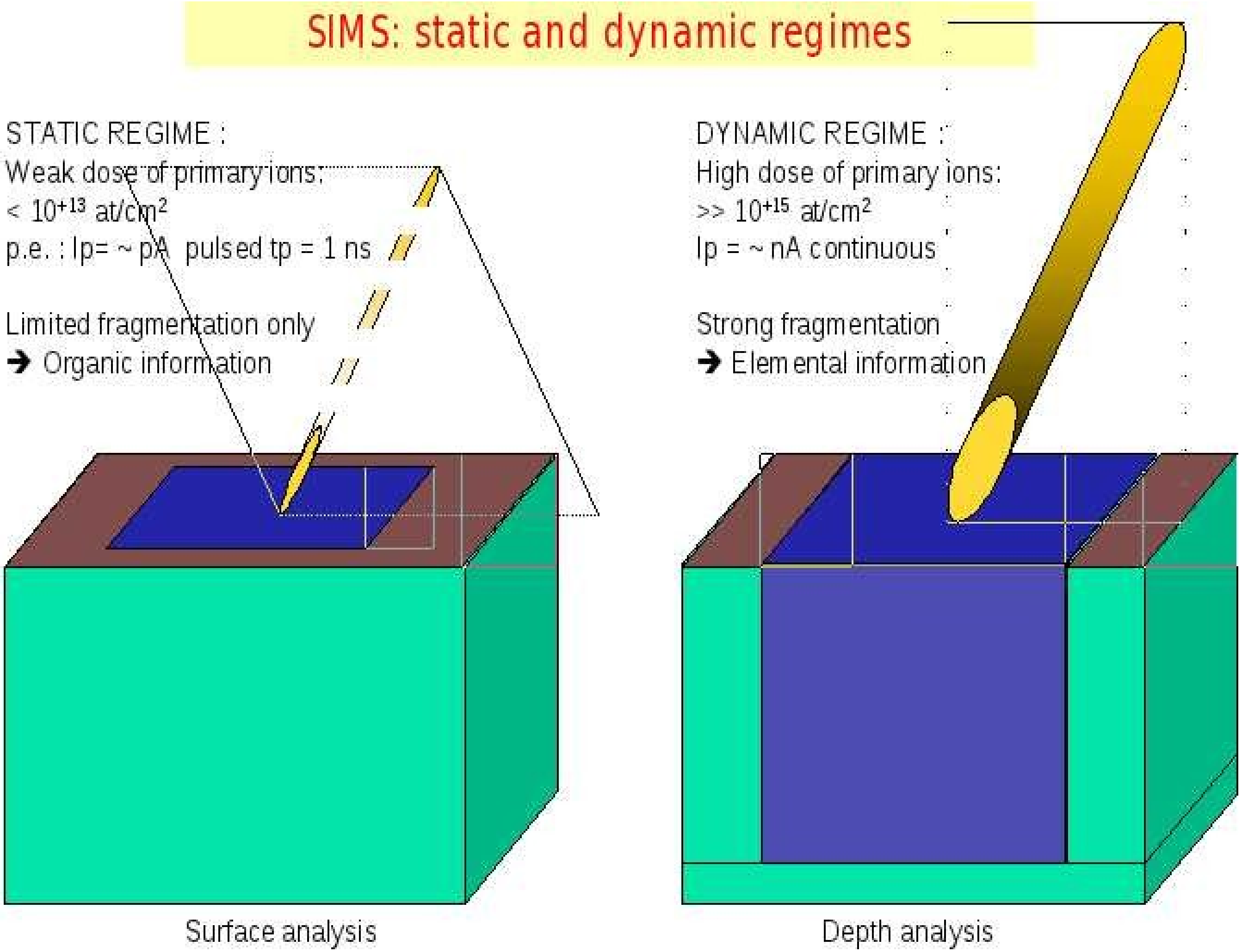

Static SIMS is the process involved in surface atomic monolayer analysis, usually with a **pulsed ion beam and a time of flight mass spectrometer**, while ***dynamic SIMS*** is the process involved in **bulk analysis**, closely related to the sputtering process, using a DC primary ion beam and a **magnetic sector or quadrupole mass spectrometer**.

Instrumentation

SIMS Manufactures

Dynamic SIMS

- Cameca (France) : magnetic sector and quadrupole
- PHI (USA/Japan) : quadrupole

Static SIMS

- Ion-Tof (Germany) : time-of-flight
- PHI (USA/Japan) : time-of-flight

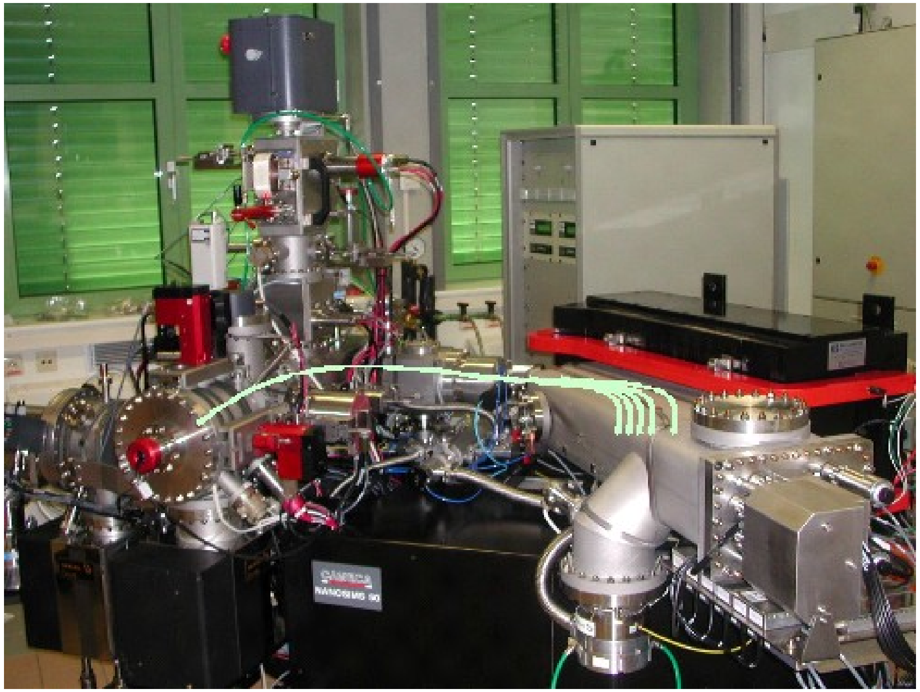

Instrumentation

dynamic SIMS

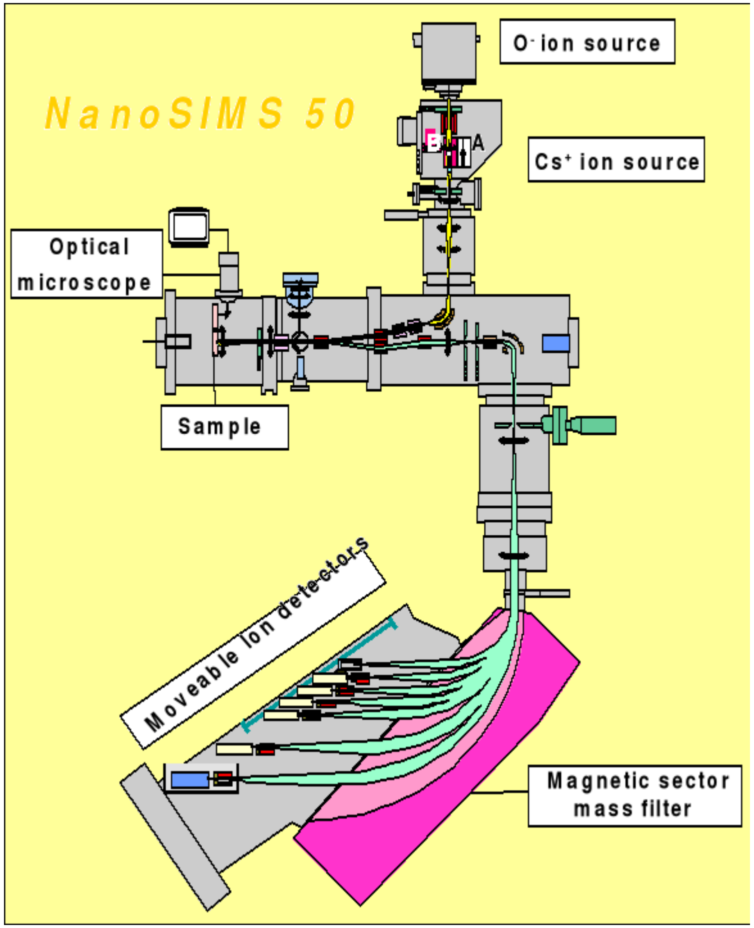

Cameca NanoSIMS 50

High resolution imaging

Primary ion guns:	Cesium, oxygen
Spatial resolution (X,Y):	50 nm (negative secondary ions), 200 nm (positive secondary ions)
Depth resolution:	nm range (not optimized)
Detection limits:	ppb to ppm until 100%
Elemental range:	H to U
Unique advantages:	High spatial resolution (< 50nm) High transmission at high mass resolution Parallel collection of 5-7 ionic species

Instrumentation

static SIMS

Ion-Tof TOF SIMS 5

Tof-SIMS for extreme surface analysis of organics

Primary ion guns: Cesium, argon, gallium, bismuth, C_{60}, Au

Spatial resolution (X,Y): 100 nm

Depth resolution: 1 nm (low-energy ion bombardment)

Detection limits: less good than dynamic SIMS (matter is lost during sputter-anaylsis cycles

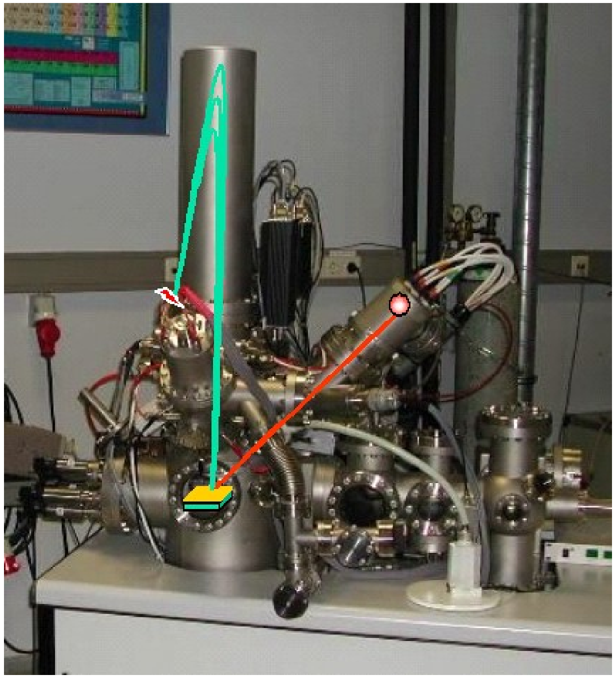

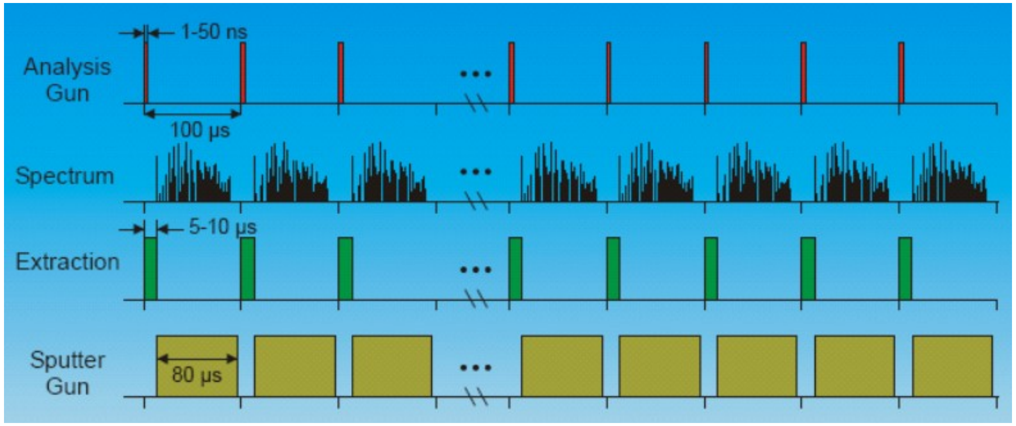

Application

Depth profiling

- recording of selected signals with respect to the sputtering time
- parallel detection or cycling between masses
- conversion between sputtering time and depth
  (measurement of the crater depth by profilometry, calculation of the erosion speed, …)
- depth resolution depending on several parameters:
  - sample (chemical composition, cristallinity, surface topography, …)
  - nature of primary ions (light or heavy ions, cluster ions, …)
  - impact energy and angle of incidence of the primary ions
  - sample rotation
  - oxygen flooding
  - focussing and rastering of the ion beam

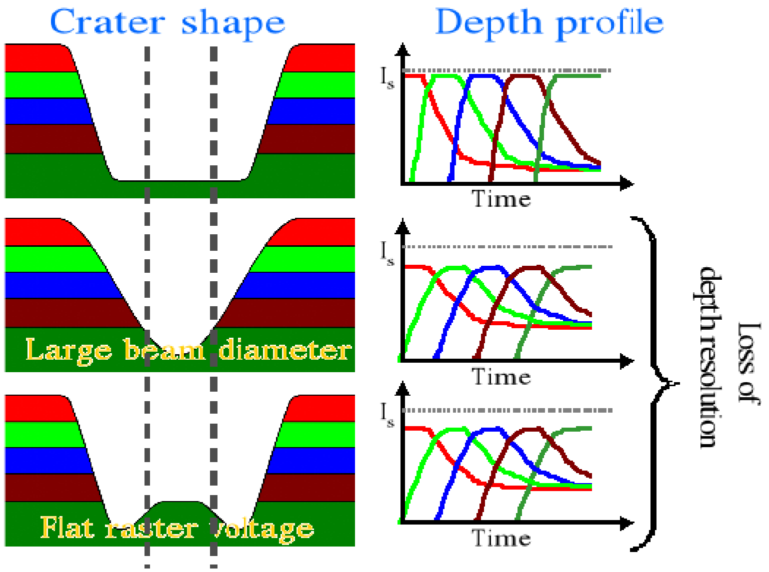

Applications

Si doping

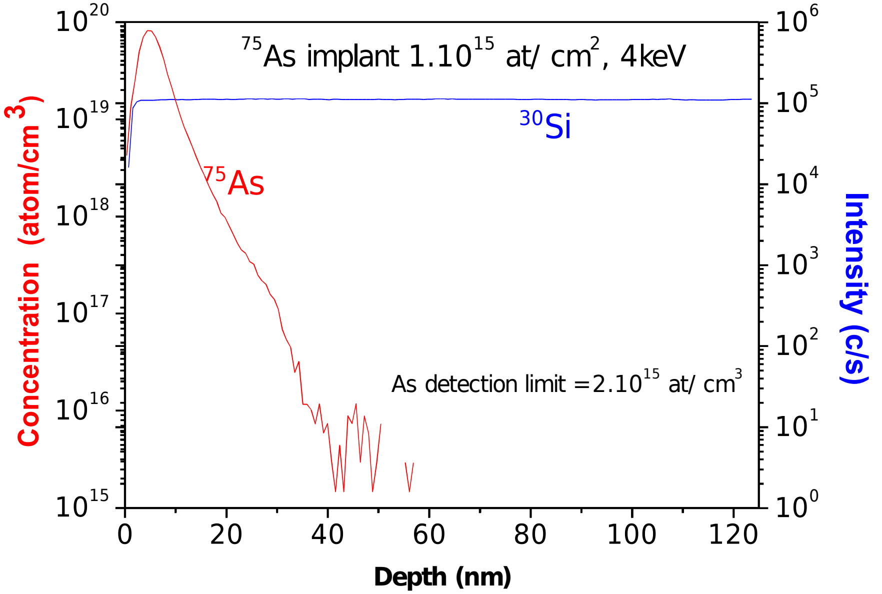

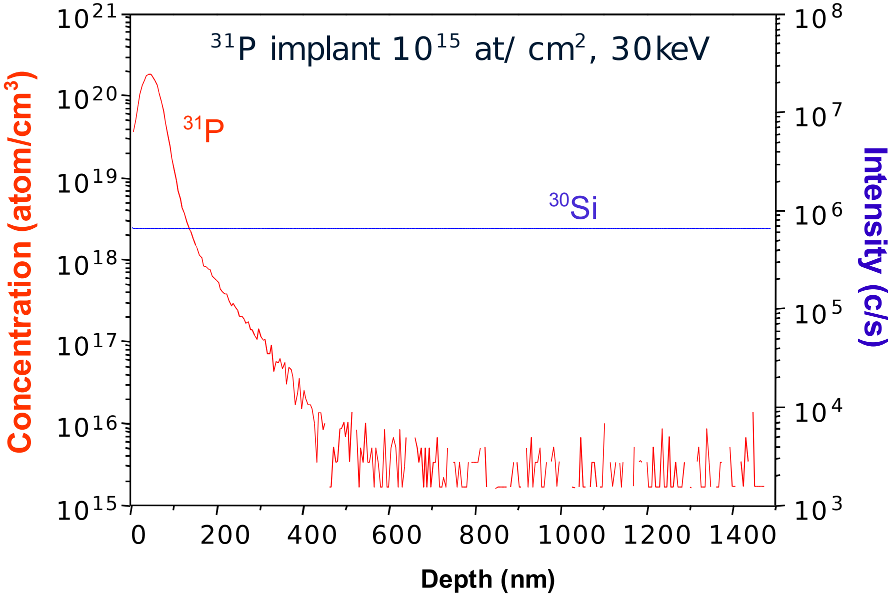

As implanted into Si
Cs^{+} primary ions at 500eV
impact energy

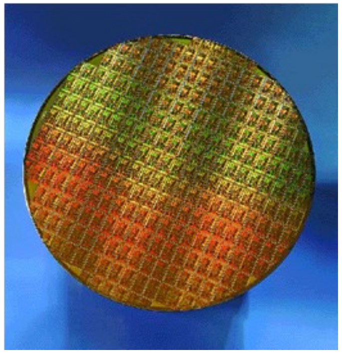

P implanted into Si
Cs^{+} primary ions at 2keV
impact energy

Application

organic solar cell

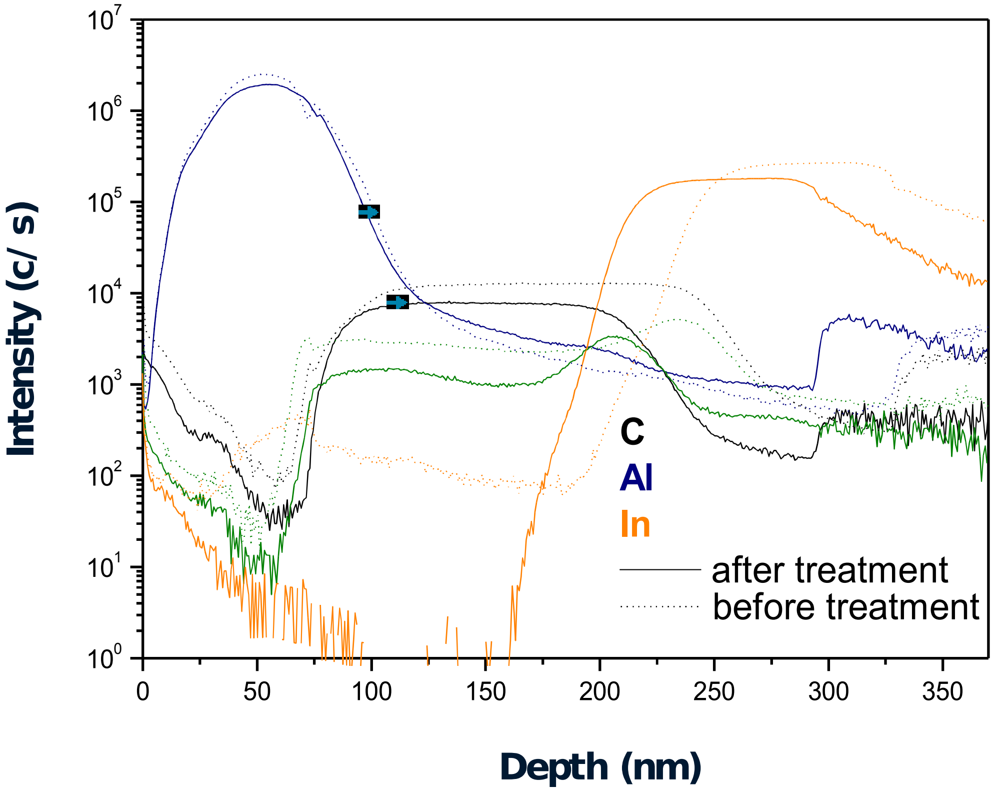

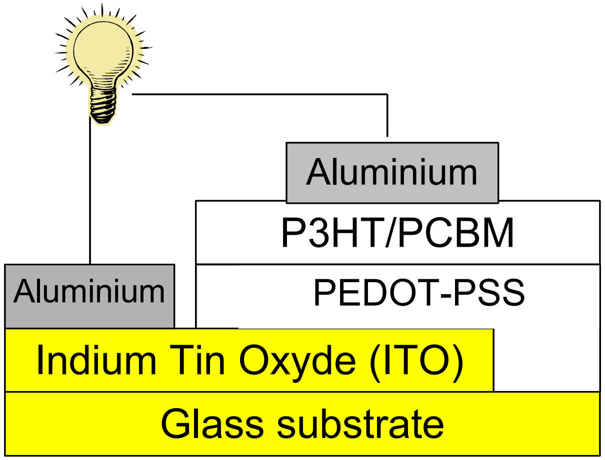

Aluminium

P3HT/PCBM

Aluminium

PEDOT-PSS

Indium Tin Oxyde (ITO)

Glass substrate

Determination of the diffusion of metallic Al in a polymer layer after heat treatment

Applications

2D imaging

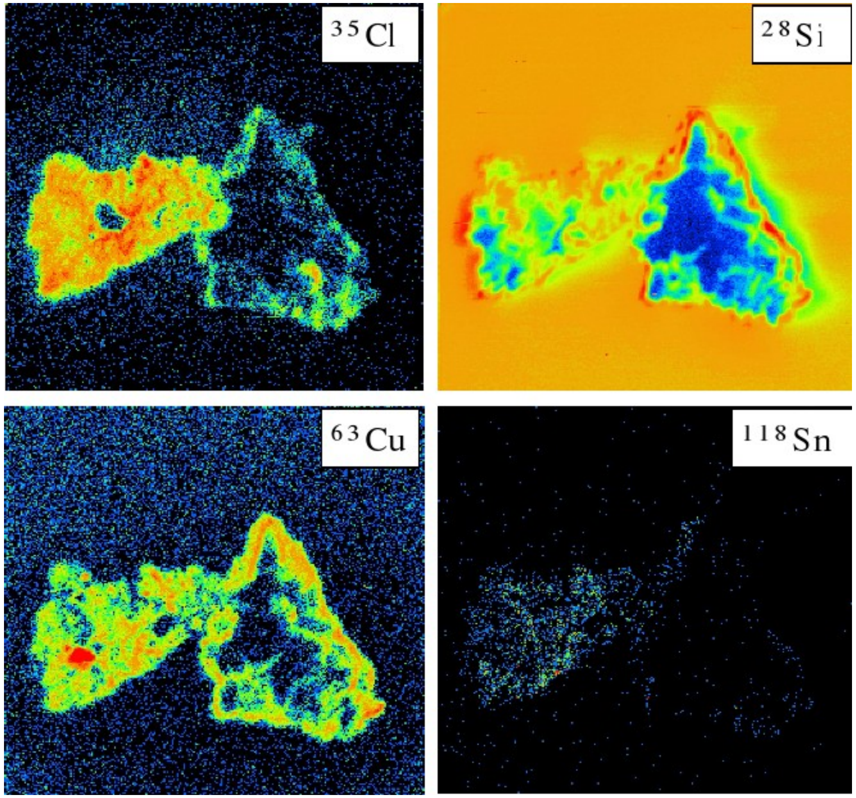

Atmospheric particles
Analyzed area : (12 x 12) µm^2

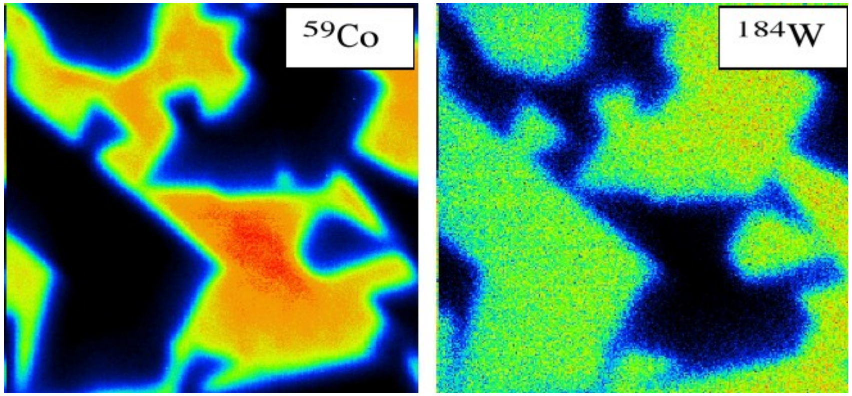

Tungsten carbide
Analyzed area : (10 x 10) µm^2

Applications
2D imaging

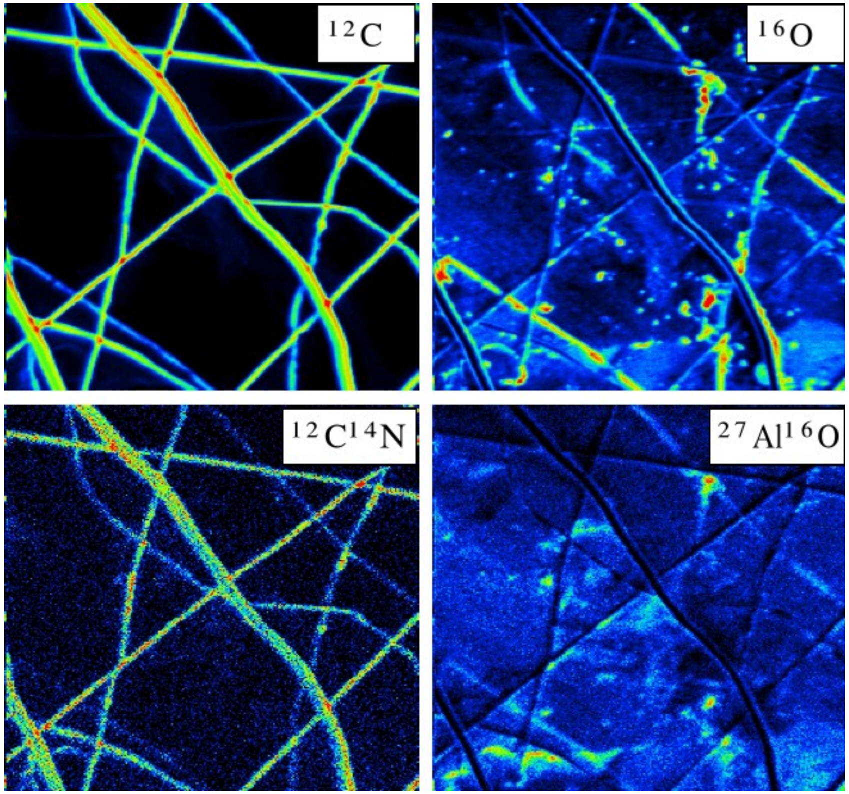

Nanofibres
Analyzed area : (10 x 10) µm^2

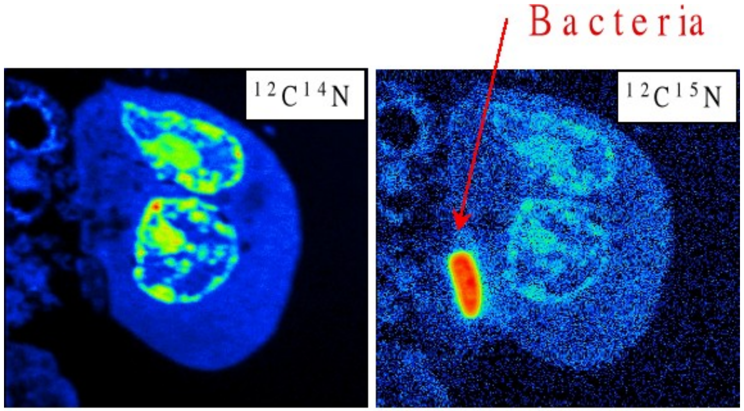

Analyzed area : (12 x 12) µm^2

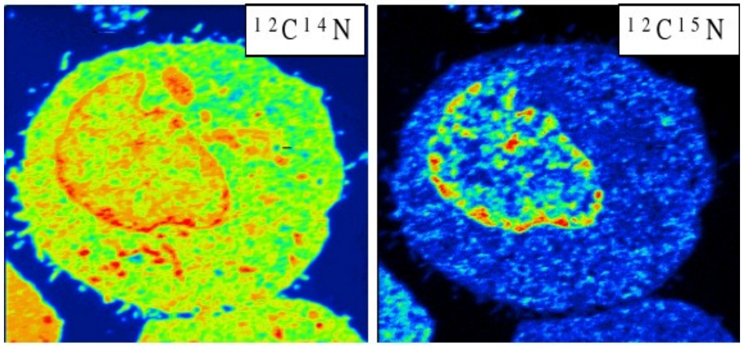

Analyzed area : (13 x 13) µm^2

E.coli labelled with ^{15}N, destroyed by the immune system

Applications

3D imaging - Polystyrene – PMMA blend

- acquisition of successive images for selected secondary ions
- depth calibration to determine the depth of origin of the different image planes
- reconstruction of the 3D image

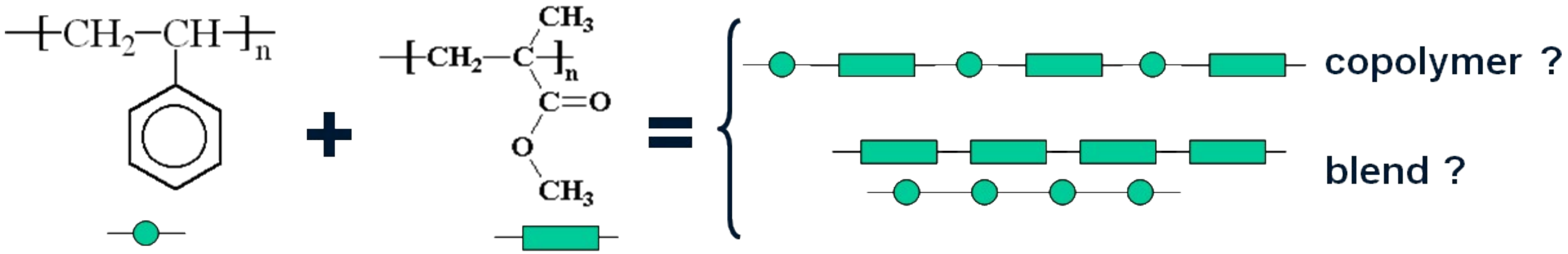

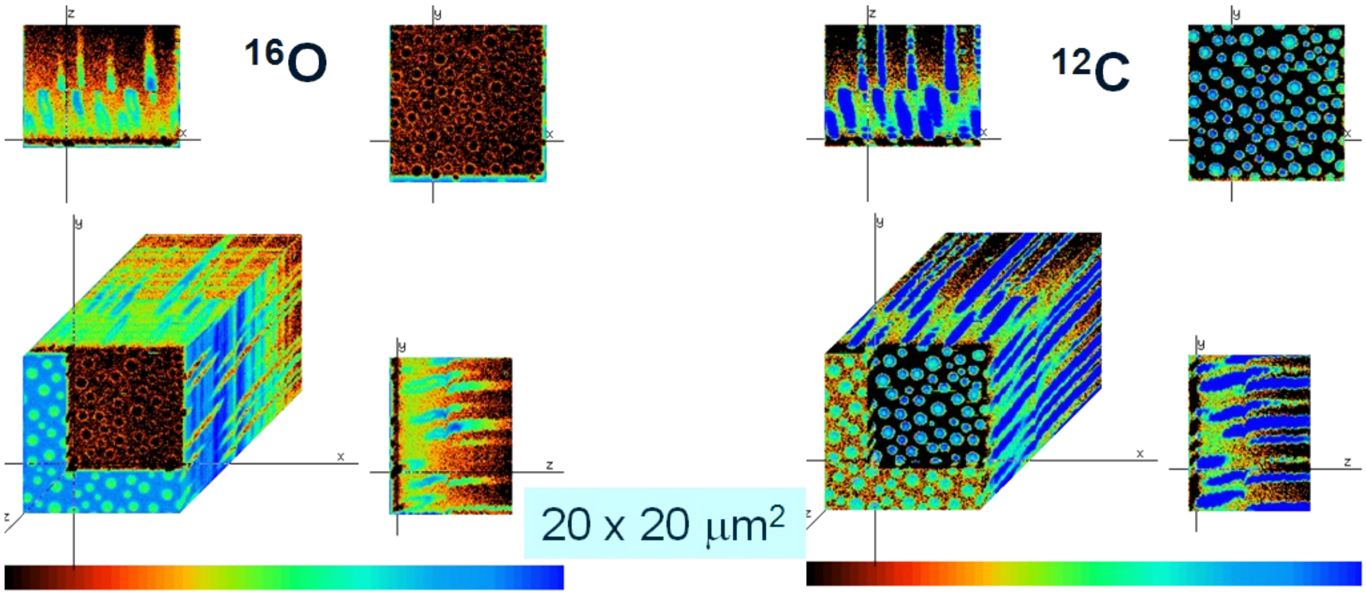

Summary

Strong points:
- all elements/isotopes detectable
- excellent sensitivity (ppm – ppb to 100%)
- high dynamic range (intensity variations can be followed over several orders of magnitude)
- high mass resolution (M/DM up to 10.000)
- isotopic measurements
- high depth resolution (1 nm at low-energy ion bombardment)
- high lateral resolution (50 nm on the Cameca NanoSIMS)
- organic information in static mode

Weak points:
- difficult to quantify measurements (« matrix effect »)

New Instrumentation

combination AFM/KPFM-SIMS!

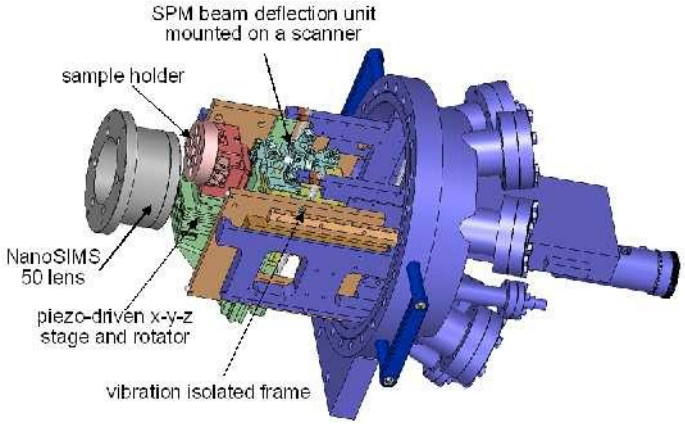

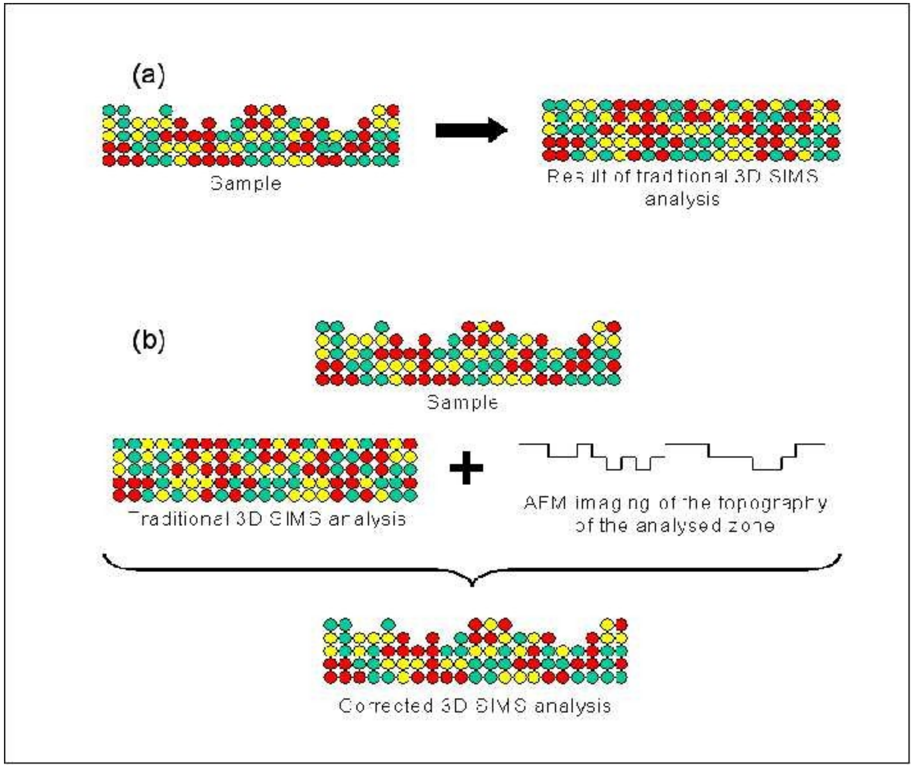

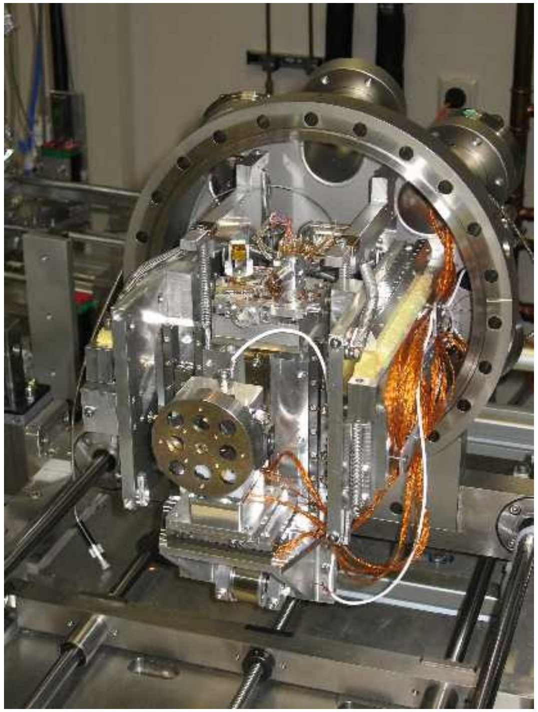

cooperation CRP - Uni Basel

T. Wirtz et al., Rev. Sci. Instrum. 83, 063702, (2012).